(32) Kuno, A.; Ikehara, Y.; Tanaka, Y.; Angata, T.; Unno, S.; Sogabe, M.; Ozaki, H.; Ito, K.; Hirabayashi, J.; Mizokami, M.; Narimatsu, H. Multilectin assay for detecting fibrosis-specific glyco-alteration by means of lectin microarray. *Clin. Chem.* **2011**, *57* (1), 48–56.
(33) Tateno, H.; Nakamura-Tsuruta, S.; Hirabayashi, J. Comparative analysis of core-fucose-binding lectins from Lens culinaris and Pisum sativum using frontal affinity chromatography. *Glycobiology* **2009**, *19* (5), 527–36.
(34) Masuzaki, R.; Karp, S. J.; Omata, M. New serum markers of hepatocellular carcinoma. *Semin. Oncol.* **2012**, *39* (4), 434–9.
(35) Yusa, A.; Miyazaki, K.; Kimura, N.; Izawa, M.; Kannagi, R. Epigenetic silencing of the sulfate transporter gene DTDST induces sialyl Lewisx expression and accelerates proliferation of colon cancer cells. *Cancer Res.* **2010**, *70* (10), 4064–73.
(36) Mizuguchi, S.; Inoue, K.; Iwata, T.; Nishida, T.; Izumi, N.; Tsukioka, T.; Nishiyama, N.; Uenishi, T.; Suehiro, S. High serum concentrations of Sialyl Lewisx predict multilevel N2 disease in non-small-cell lung cancer. *Ann. Surg. Oncol.* **2006**, *13* (7), 1010–8.
(37) Peracaula, R.; Tabares, G.; Lopez-Ferrer, A.; Brossmer, R.; de Bolos, C.; de Llorens, R. Role of sialyltransferases involved in the biosynthesis of Lewis antigens in human pancreatic tumour cells. *Glycoconjugate J.* **2005**, *22* (3), 135–44.
(38) Lee, J. K.; Bistrup, A.; van Zante, A.; Rosen, S. D. Activities and expression pattern of the carbohydrate sulfotransferase GlcNAc6ST-3 (I-GlcNAc6ST): functional implications. *Glycobiology* **2003**, *13* (4), 245–54.
(39) Taketa, K.; Ichikawa, E.; Sakuda, H.; Iwamasa, T.; Hayakawa, M.; Taga, H.; Hirai, H. Lectin reactivity of alpha-fetoprotein in a case of renal cell carcinoma. *Tumour Biol,* **1989**, *10* (5), 275–80.
(40) Medical devices; immunology and microbiology devices; classification of AFP-L3% immunological test systems. Final rule. *Fed. Regist.* **2005**, *70* (191), 57748–50.
(41) Zhao, Y.; Jia, W.; Wang, J.; Ying, W.; Zhang, Y.; Qian, X. Fragmentation and site-specific quantification of core fucosylated glycoprotein by multiple reaction monitoring-mass spectrometry. *Anal. Chem.* **2011**, *83* (22), 8802–9.
(42) Comunale, M. A.; Lowman, M.; Long, R. E.; Krakover, J.; Philip, R.; Seeholzer, S.; Evans, A. A.; Hann, H. W.; Block, T. M.; Mehta, A. S. Proteomic analysis of serum associated fucosylated glycoproteins in the development of primary hepatocellular carcinoma. *J. Proteome Res.* **2006**, *5* (2), 308–15.
(43) Marrero, J. A.; Feng, Z.; Wang, Y.; Nguyen, M. H.; Befeler, A. S.; Roberts, L. R.; Reddy, K. R.; Harnois, D.; Llovet, J. M.; Normolle, D.; Dalhgren, J.; Chia, D.; Lok, A. S.; Wagner, P. D.; Srivastava, S.; Schwartz, M. Alpha-fetoprotein, des-gamma carboxyprothrombin, and lectin-bound alpha-fetoprotein in early hepatocellular carcinoma. *Gastroenterology* **2009**, *137* (1), 110–8.
(44) Tan, F.; Weerasinghe, D. K.; Skidgel, R. A.; Tamei, H.; Kaul, R. K.; Roninson, I. B.; Schilling, J. W.; Erdos, E. G. The deduced protein sequence of the human carboxypeptidase N high molecular weight subunit reveals the presence of leucine-rich tandem repeats. *J. Biol. Chem.* **1990**, *265* (1), 13–9.
(45) Wang, Z. E.; Myles, G. M.; Brandt, C. S.; Lioubin, M. N.; Rohrschneider, L. Identification of the ligand-binding regions in the macrophage colony-stimulating factor receptor extracellular domain. *Mol. Cell. Biol.* **1993**, *13* (9), 5348–59.
(46) Mitchell, P. Proteomics retrenches. *Nat. Biotechnol.* **2010**, *28* (7), 665–70.
(47) Rosenberg, W. M.; Voelker, M.; Thiel, R.; Becka, M.; Burt, A.; Schuppan, D.; Hubscher, S.; Roskams, T.; Pinzani, M.; Arthur, M. J. Serum markers detect the presence of liver fibrosis: a cohort study. *Gastroenterology* **2004**, *127* (6), 1704–13.
(48) Kuno, A.; Ikehara, Y.; Tanaka, Y.; Saito, K.; Ito, K.; Tsuruno, C.; Nagai, S.; Takahama, Y.; Mizokami, M.; Hirabayashi, J.; Narimatsu, H. LecT-Hepa: A triplex lectin-antibody sandwich immunoassay for estimating the progression dynamics of liver fibrosis assisted by a bedside clinical chemistry analyzer and an automated pretreatment machine. *Clin. Chim. Acta* **2011**, *412* (19–20), 1767–72.
(49) Du, D.; Zhu, X.; Kuno, A.; Matsuda, A.; Tsuruno, C.; Yu, D.; Zhang, Y.; Ikehara, Y.; Tanaka, Y.; Zhang, X.; Narimatsu, H. Comparison of LecT-Hepa and FibroScan for assessment of liver fibrosis in hepatitis B virus infected patients with different ALT levels. *Clin. Chim. Acta* **2012**, *413* (21–22), 1796–9.
(50) Lau, C. P.; Poon, R. T.; Cheung, S. T.; Yu, W. C.; Fan, S. T. SPARC and Hevin expression correlate with tumour angiogenesis in hepatocellular carcinoma. *J. Pathol.* **2006**, *210* (4), 459–68.

HEPATOLOGY
Official Journal of the American Association for the Study of Liver Diseases

Human Blood Dendritic Cell Antigen 3 (BDCA3)$^+$ Dendritic Cells Are a Potent Producer of Interferon-λ in Response to Hepatitis C Virus

Sachiyo Yoshio,[1] Tatsuya Kanto,[1] Shoko Kuroda,[1] Tokuhiro Matsubara,[1] Koyo Higashitani,[1] Naruyasu Kakita,[1] Hisashi Ishida,[1] Naoki Hiramatsu,[1] Hiroaki Nagano,[2] Masaya Sugiyama,[3] Kazumoto Murata,[3] Takasuke Fukuhara,[4] Yoshiharu Matsuura,[4] Norio Hayashi,[5] Masashi Mizokami,[3] and Tetsuo Takehara[1]

The polymorphisms in the interleukin (*IL)-28B* (interferon-lambda [IFN]-λ3) gene are strongly associated with the efficacy of hepatitis C virus (HCV) clearance. Dendritic cells (DCs) sense HCV and produce IFNs, thereby playing some cooperative roles with HCV-infected hepatocytes in the induction of interferon-stimulated genes (ISGs). Blood dendritic cell antigen 3 (BDCA3)$^+$ DCs were discovered as a producer of IFN-λ upon Toll-like receptor 3 (TLR3) stimulation. We thus aimed to clarify the roles of BDCA3$^+$ DCs in anti-HCV innate immunity. Seventy healthy subjects and 20 patients with liver tumors were enrolled. BDCA3$^+$ DCs, in comparison with plasmacytoid DCs and myeloid DCs, were stimulated with TLR agonists, cell-cultured HCV (HCVcc), or Huh7.5.1 cells transfected with HCV/JFH-1. BDCA3$^+$ DCs were treated with anti-CD81 antibody, inhibitors of endosome acidification, TIR-domain-containing adapter-inducing interferon-β (TRIF)-specific inhibitor, or ultraviolet-irradiated HCVcc. The amounts of IL-29/IFN-λ1, IL-28A/IFN-λ2, and IL-28B were quantified by subtype-specific enzyme-linked immunosorbent assay (ELISA). The frequency of BDCA3$^+$ DCs in peripheral blood mononuclear cell (PBMC) was extremely low but higher in the liver. BDCA3$^+$ DCs recovered from PBMC or the liver released large amounts of IFN-λs, when stimulated with HCVcc or HCV-transfected Huh7.5.1. BDCA3$^+$ DCs were able to induce ISGs in the coexisting JFH-1-positive Huh7.5.1 cells. The treatments of BDCA3$^+$ DCs with anti-CD81 antibody, cloroquine, or bafilomycin A1 reduced HCVcc-induced IL-28B release, whereas BDCA3$^+$ DCs comparably produced IL-28B upon replication-defective HCVcc. The TRIF-specific inhibitor reduced IL-28B release from HCVcc-stimulated BDCA3$^+$ DCs. In response to HCVcc or JFH-1-Huh7.5.1, BDCA3$^+$ DCs in healthy subjects with IL-28B major (rs8099917, TT) released more IL-28B than those with IL-28B minor genotype (TG). *Conclusion*: Human BDCA3$^+$ DCs, having a tendency to accumulate in the liver, recognize HCV in a CD81-, endosome-, and TRIF-dependent manner and produce substantial amounts of IL-28B/IFN-λ3, the ability of which is superior in subjects with IL-28B major genotype. (HEPATOLOGY 2013;57:1705-1715)

Hepatitis C virus (HCV) infection is one of the most serious health problems in the world. More than 170 million people are chronically infected with HCV and are at high risk of developing liver cirrhosis and hepatocellular carcinoma. Genome-wide association studies have successfully identified the genetic polymorphisms (single nucleotide polymorphisms, SNPs) upstream of the promoter region of the

Abbreviations: Ab, antibody; HCV, hepatitis C virus; HCVcc, cell-cultured hepatitis C virus; HSV, herpes simplex virus; IHL, intrahepatic lymphocyte; INF-λ, interferon-lambda; IRF, interferon regulatory factor; ISGs, interferon-stimulated genes; JEV, Japanese encephalitis virus; Lin, lineage; mDC, myeloid DC; MOI, multiplicity of infection; PBMC, peripheral blood mononuclear cell; pDC, plasmacytoid DC; Poly IC, polyinosine-polycytidylic acid; RIG-I, retinoic acid-inducible gene-I; SNPs, single nucleotide polymorphisms; TLR, Toll-like receptor; TRIF, TIR-domain-containing adapter-inducing interferon-β.

From the [1]Department of Gastroenterology and Hepatology, Osaka University Graduate School of Medicine, Osaka, Japan; [2]Department of Surgery, Osaka University Graduate School of Medicine, Osaka, Japan; [3]Research Center for Hepatitis and Immunology, National Center for Global Health and Medicine, Ichikawa, Japan; [4]Department of Molecular Virology, Research Institute for Microbial Diseases, Osaka University, Osaka, Japan; [5]Kansai Rosai Hospital, Hyogo, Japan.

Received July 2, 2012; accepted November 13, 2012.

Supported in part by a Grant-In-Aid for Scientific Research from the Ministry of Education, Culture, Sports, Science, and Technology, Japan and a Grant-In-Aid from the Ministry of Health, Labor, and Welfare of Japan.

interleukin (IL)-28B / interferon-lambda 3 (IFN-λ3) gene, which are strongly associated with the efficacy of pegylated interferon-α (PEG-IFN-α) and ribavirin therapy or spontaneous HCV clearance.[1-4]

IFN-λs, or type III IFNs, comprise a family of highly homologous molecules consisting of IFN-λ1 (IL-29), IFN-λ2 (IL-28A), and IFN-λ3 (IL-28B). In clear contrast to type I IFNs, they are released from relatively restricted types of cells, such as hepatocytes, intestinal epithelial cells, or dendritic cells (DCs). Also, the cells that express heterodimeric IFN-λ receptors (IFN-λR1 and IL-10R2) are restricted to cells of epithelial origin, hepatocytes, or DCs.[5] Such limited profiles of cells expressing IFN-λs and their receptors define the biological uniqueness of IFN-λs. It has been shown that IFN-λs convey anti-HCV activity by inducing various interferon-stimulated genes (ISGs),[5] the profiles of which were overlapped but others were distinct from those induced by IFN-α/β. Some investigators showed that the expression of IL-28 in PBMC was higher in subjects with IL-28B major than those with minor; however, the levels of IL-28 transcripts in liver tissue were comparable regardless of IL-28B genotype.[2,6]

At the primary exposure to hosts, HCV maintains high replicative levels in the infected liver, resulting in the induction of IFNs and ISGs. In a case of successful HCV eradication, it is postulated that IFN-α/β and IFN-λ cooperatively induce antiviral ISGs in HCV-infected hepatocytes. It is of particular interest that, in primary human hepatocytes or chimpanzee liver, IFN-λs, but not type I IFNs, are primarily induced after HCV inoculation, the degree of which is closely correlated with the levels of ISGs.[7] These results suggest that hepatic IFN-λ could be a principal driver of ISG induction in response to HCV infection. Nevertheless, the possibility remains that DCs, as a prominent IFN producer in the liver, play significant roles in inducing hepatic ISGs and thereby suppressing HCV replication.

DCs, as immune sentinels, sense specific genomic and/or structural components of pathogens with various pattern recognition receptors and eventually release IFNs and inflammatory cytokines.[8] In general, DCs migrate to the organ where inflammation or cellular apoptosis occurs and alter their function in order to alleviate or exacerbate the disease conditions. Therefore, the phenotypes and/or capacity of liver DCs are deemed to be influenced in the inflamed liver. In humans, the existence of phenotypically and functionally distinct DC subsets has been reported: myeloid DC (mDC) and plasmacytoid DC (pDC).[9] Myeloid DCs predominantly produce IL-12 or tumor necrosis factor alpha (TNF-α) following proinflammatory stimuli, while pDCs release considerable amounts of type I IFNs upon virus infection.[9] The other type of mDCs, mDC2 or BDCA3$^+$(CD141) DCs, have been drawing much attention recently, since human BDCA3$^+$ DCs are reported to be a counterpart of murine CD8a$^+$ DCs.[10] Of particular interest is the report that BDCA3$^+$ DCs have a potent capacity of releasing IFN-λ in response to Toll-like receptor 3 (TLR3) agonist.[11] However, it is still largely unknown whether human BDCA3$^+$ DCs are able to respond to HCV.

Taking these reports into consideration, we hypothesized that human BDCA3$^+$ DCs, as a producer of IFN-λs, have crucial roles in anti-HCV innate immunity. We thus tried to clarify the potential of BDCA3$^+$ DCs in producing type III IFNs by using cell-cultured HCV (HCVcc) or hepatoma cells harboring HCV as stimuli. Our findings show that BDCA3$^+$ DCs are quite a unique DC subset, characterized by a potent and specialized ability to secrete IFN-λs in response to HCV. The ability of BDCA3$^+$ DCs to release IL-28B upon HCV is superior in subjects with IL-28B major (rs8099917, TT) to those with minor (TG or GG) genotype, suggesting that BDCA3$^+$ DCs are one of the key players in IFN-λ-mediated innate immunity.

Patients and Methods

Subjects. This study enrolled 70 healthy volunteers (male/female: 61/9) (age: mean ± standard deviation [SD], 37.3 ± 7.8 years) and 20 patients who underwent surgical resection of liver tumors at Osaka University Hospital (Supporting Table 1). The study was approved by the Ethical Committee of Osaka University Graduate School of Medicine. Written informed consent was obtained from all of them. All healthy volunteers were negative for HCV, hepatitis B virus (HBV), and human immunodeficiency virus (HIV) and had no apparent history of liver, autoimmune, or malignant diseases.

Address reprint requests to: Tatsuya Kanto, M.D., Ph.D., Department of Gastroenterology and Hepatology, Osaka University Graduate School of Medicine, 2-2 Yamadaoka, Suita, 565-0871 Japan. E-mail: kantot@gh.med.osaka-u.ac.jp; fax: +81-6-6879-3629.

View this article online at wileyonlinelibrary.com.

DOI 10.1002/hep.26182

Potential conflict of interest: Nothing to report.

Additional Supporting Information may be found in the online version of this article.

Reagents. The specifications of all antibodies used for FACS or cell sorting TLR-specific synthetic agonists, pharmacological reagents, and inhibitory peptides are listed in the Supporting Materials.

Separation of DCs from PBMC or Intrahepatic Lymphocytes. We collected 400 mL of blood from each healthy volunteer and processed them for PBMCs. Noncancerous liver tissues were obtained from patients who underwent resection of liver tumors (Supporting Table 1). For the collection of intrahepatic lymphocytes (IHLs), liver tissues were washed thoroughly with phosphate-buffered saline to remove the peripheral blood adhering to the tissue and ground gently. After Lin-negative ($CD3^-$, $CD14^-$, $CD19^-$, and $CD56^-$) cells were obtained by the MACS system, each DC subset with the defined phenotype was sorted separately under FACS Aria (BD). The purity was more than 98%, as assessed by FACS Canto II (BD). Sorted DCs were cultured at 2.5×10^4/well on 96-well culture plates.

Immunofluorescence Staining of Human Liver Tissue. Tissue specimens were obtained from surgical resections of noncancerous liver from the patients as described above. Briefly, the 5-mm sections were incubated with the following antibodies: mouse biotinylated antihuman BDCA3 antibody (Miltenyi-Biotec), and mouse antihuman CLEC9A antibody (Biolegend) and subsequently with secondary goat antirabbit Alexa Fluor488 or goat antimouse Alexa Fluor594 (Invitrogen, Molecular Probes) antibodies. Cell nuclei were counterstained with Dapi-Fluoromount-GTM (Southern Biotech, Birmingham, AL). The stained tissues were analyzed by fluorescence microscopy (Model BZ-9000; Keyence, Osaka, Japan).

Cells and Viruses. The *in vitro* transcribed RNA of the JFH-1 strain of HCV was introduced into FT3-7 cells[12] or Huh7.5.1 cells. The stocks of HCVcc were generated by concentration of the medium from JFH-1-infected FT3-7 cells. The virus titers were determined by focus forming assay.[13] The control medium was generated by concentration of the medium from HCV-uninfected FT3-7 cells. Infectious JEVs were generated from the expression plasmid (pMWJEATG1) as reported.[14] HSV (KOS) was a generous gift from Dr. K. Ueda (Osaka University). Huh7.5.1 cells transduced with HCV JFH-1 strain was used for the coculture with DCs. The transcripts of ISGs in Huh7.5.1 were examined by reverse-transcription polymerase chain reaction (RT-PCR) methods using gene-specific primers and probes (Applied Biosystems, Foster City, CA).

Secretion Assays. IL-28B/IFN-λ3 was quantified by a newly developed chemiluminescence enzyme immunoassay (CLEIA) system.[15] IL-29/IFN-λ1, IL-28A/IFN-λ2, and IFN-β were assayed by commercially available enzyme-linked immunosorbent assay (ELISA) kits (eBioscience, R&D, and PBL, respectively). IFN-α was measured by cytometric beads array kits (BD) according to the manufacturer's instructions.

Statistical Analysis. The differences between two groups were assessed by the Mann-Whitney nonparametric *U* test. Multiple comparisons between more than two groups were analyzed by the Kruskal-Wallis nonparametric test. Paired *t* tests were used to compare differences in paired samples. All the analyses were performed using GraphPad Prism software (San Diego, CA).

Results

Human BDCA3$^+$ DCs Are Phenotypically Distinct from pDCs and mDCs. We defined BDCA3$^+$ DCs as $Lin^-HLA\text{-}DR^+BDCA3^{high+}$ cells (Fig. 1A, left, middle), and pDCs and mDCs by the patterns of CD11c and CD123 expressions (Fig. 1A, right). The level of CD86 on pDCs or mDCs is comparatively higher than those on BDCA3$^+$ DCs (Fig. 1B). The expression of CD81 is higher on BDCA3$^+$ DCs than on pDCs and mDCs (Fig. 1B, Supporting Fig. S1). CLEC9A, a member of C-type lectin, is expressed specifically on BDCA3$^+$ DCs as reported elsewhere,[16] but not on pDCs and mDCs (Fig. 1B).

Liver BDCA3$^+$ DCs Are More Mature than the Counterparts in the Periphery. BDCA3$^+$ DCs in infiltrated hepatic lymphocytes (IHLs) are all positive for CLEC9A, but liver pDCs or mDCs are not (data not shown). The levels of CD40, CD80, CD83, and CD86 on liver BDCA3$^+$ DCs are higher than those on the peripheral counterparts, suggesting that BDCA3$^+$ DCs are more mature in the liver compared to those in the periphery (Fig. 1C).

In order to confirm that BDCA3$^+$ DCs are localized in the liver, we stained the cells with immunofluorescence antibodies (Abs) in noncancerous liver tissues. Liver BDCA3$^+$ DCs were defined as BDCA3$^+$ CLEC9A$^+$ cells (Fig. 1D). Most of the cells were found near the vascular compartment or in sinusoid or the space of Disse of the liver tissue.

BDCA3$^+$ DCs Are Scarce in PBMCs but More Abundant in the Liver. The percentages of BDCA3$^+$ DCs in PBMCs were much lower than those of the other DC subsets (BDCA3$^+$ DCs, pDCs and mDCs, mean $\pm$ SD [%], 0.054 ± 0.044, 0.27 ± 0.21 and 1.30 ± 0.65) (Fig. 2A). The percentages of BDCA3$^+$ DCs in IHLs were lower than those of the others (BDCA3$^+$ DCs, pDCs, and mDCs, mean $\pm$ SD [%],

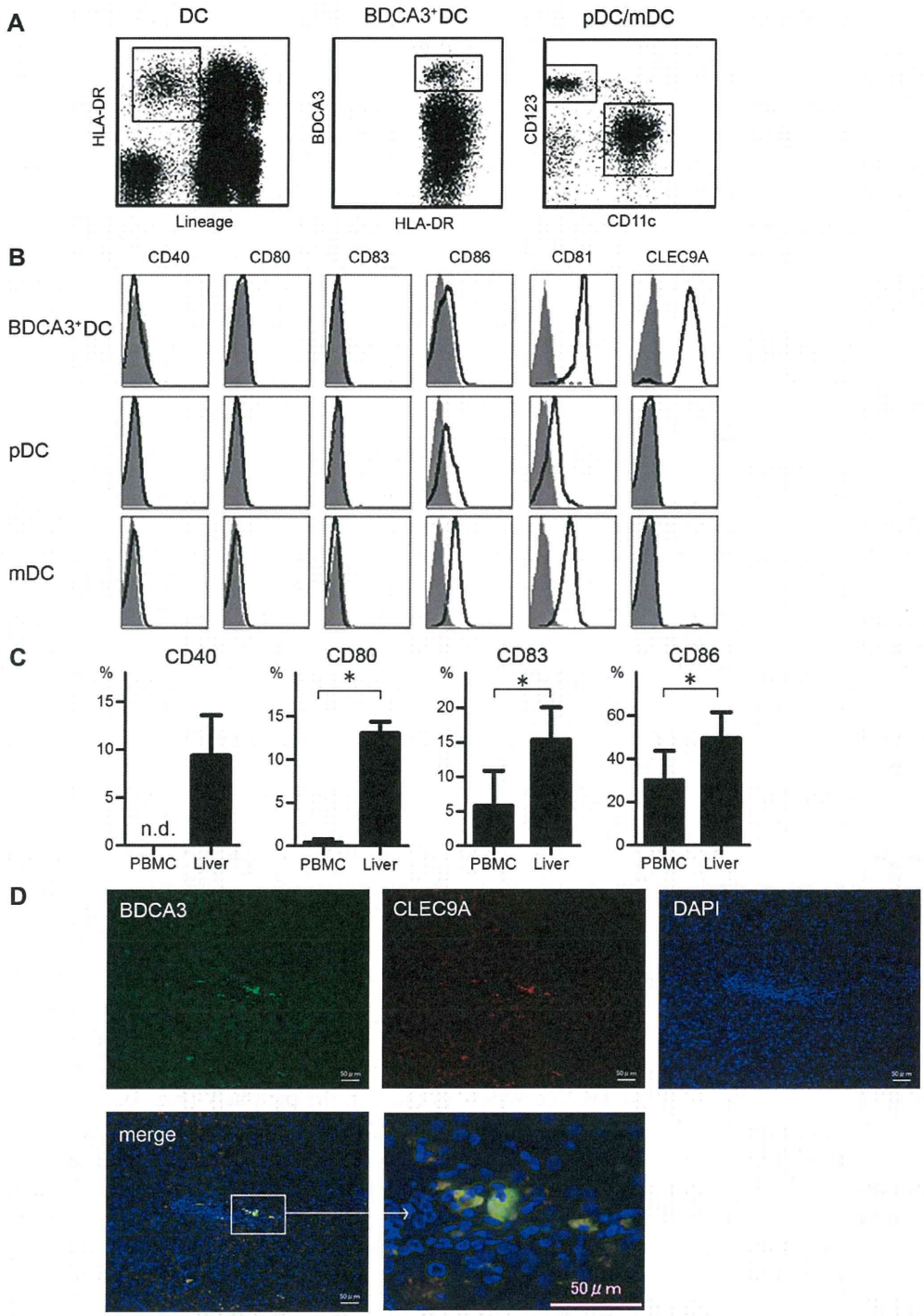

Fig. 1. Identification and phenotypic analyses of peripheral blood and intrahepatic BDCA3$^+$ DCs. (A) We defined BDCA3$^+$ DCs as Lineage$^-$HLA-DR$^+$BDCA3^{high+} cells (middle), pDCs as Lineage$^-$HLA-DR$^+$CD11c$^-$CD123^{high+} cells, and mDCs as Lineage$^-$HLA-DR$^+$CD11c$^+$CD123^{low+} cells (right). (B) The expressions of CD40, CD80, CD83, CD86, CD81, and CLEC9A on each DC subset in peripheral blood are shown. Representative results of five donors are shown in the histograms. Filled gray histograms depict data with isotype Abs, and open black ones are those with specific Abs. (C) The expressions of costimulatory molecules on BDCA3$^+$ DCs were compared between in PBMCs and in the liver. The results are shown as the percentage of positive cells. Results are the mean ± SEM from four independent experiments. *$P < 0.05$ by paired t test. (D) The staining for BDCA3 (green), CLEC9A (red) identifies BDCA3$^+$ DCs (merge, BDCA3$^+$CLEC9A$^+$) in human liver tissues. Representative results of the noncancerous liver samples are shown. BDCA, blood dendritic cell antigen; pDC, plasmacytoid DC; mDC, myeloid DC; CLEC9A, C-type lectin 9A.

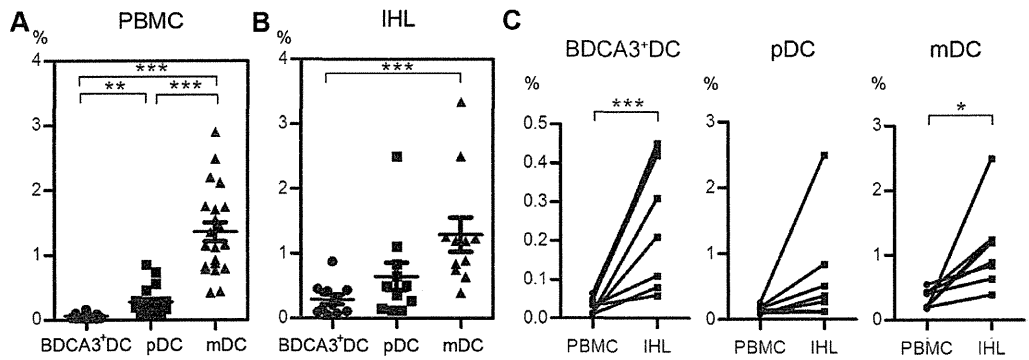

Fig. 2. Analysis of frequency of DC subsets in the peripheral blood and in the liver. Frequencies of BDCA3$^+$ DCs, pDCs, and mDCs in PBMCs (21 healthy subjects) (A) or in the intrahepatic lymphocytes (IHLs) (11 patients who had undergone surgical resection of tumors) (B) are shown. Horizontal bars depict the mean ± SD. $^{**}P < 0.005$; $^{***}P < 0.0005$ by Kruskal-Wallis test. (C) The paired comparisons of the frequencies of DC subsets between in PBMCs and in IHLs. the results of eight patients whose PBMCs and IHLs were obtained simultaneously are shown. $^{*}P < 0.05$; $^{***}P < 0.0005$ by paired *t* test. IHLs, intrahepatic lymphocytes; pDC and mDC, see Fig. 1.

0.29 ± 0.25, 0.65 ± 0.69 and 1.2 ± 0.94) (Fig. 2B). The percentages of BDCA3$^+$ DCs in the IHLs were significantly higher than those in PBMCs from relevant donors (Fig. 2C). Such relative abundance of BDCA3$^+$ DCs in the liver over that in the periphery was observed regardless of the etiology of the liver disease (Supporting Table 1).

BDCA3$^+$ DCs Produce a Large Amount of IFN-λs upon Poly IC Stimulation. We compared DC subsets for their abilities to produce IL-29/IFN-λ1, IL-28A/IFN-λ2, IL-28B/IFN-λ3, IFN-β, and IFN-α in response to TLR agonists. Approximately 4.0×10^4 of BDCA3$^+$ DCs were recoverable from 400 mL of donated blood from healthy volunteers. We fixed the number of DCs at 2.5×10^4 cells/100 mL for comparison in the following experiments.

BDCA3$^+$ DCs have been reported to express mRNA for TLR1, 2, 3, 6, 8, and 10.[17] First, we quantified IL-28B/IFN-λ3 as a representative for IFN-λs after stimulation of BDCA3$^+$ DCs with relevant TLR agonists. We confirmed that BDCA3$^+$ DCs released IL-28B robustly in response to TLR3 agonist/poly IC but not to other TLR agonists (Fig. S2). In contrast, pDCs produced IL-28B in response to TLR9 agonist/CpG but much lesser to other agonists (Fig. S2). Next, we compared the capabilities of DCs inducing IFN-λs and IFN-β genes in response to relevant TLR agonists. BDCA3$^+$ DCs expressed extremely high levels of IL-29, IL-28A, and IL-28B transcripts compared to other DCs, whereas pDCs induced a higher level of IFN-β than other DCs (Fig. S3A).

Similar results were obtained with the protein levels of IFN-λs, IFN-β, and IFN-α released from DC subsets stimulated with TLR agonists. BDCA3$^+$ DCs produce significantly higher levels of IL-29, IL-28B, and IL-28A than the other DC subsets. In clear contrast, pDCs release a significantly larger amount of IFN-β and IFN-α than BDCA3$^+$ DCs or mDCs (Fig. 3A, Fig. S3B). As for the relationship among the quantity of IFN-λ subtypes from poly IC-stimulated BDCA3$^+$ DCs, the levels of IL-29/IFN-λ1 and IL-28B/IFN-λ3 were positively correlated ($R^2 = 0.76$, $P < 0.05$), and those of IL-28A/IFN-λ2 and IL-28B/IFN-λ3 were positively correlated as well ($R^2 = 0.84$, $P < 0.0005$), respectively (Fig. S3C). These results show that the transcription and translation machineries of IFN-λs may be overlapped among IFN-λ subtypes in BDCA3$^+$ DCs upon poly IC stimulation.

Liver BDCA3$^+$ DCs sorted from IHLs possess the ability to produce IL-28B in response to poly IC (Fig. 3B), showing that they are comparably functional. In response to poly IC, BDCA3$^+$ DCs were capable of producing inflammatory cytokines as well, such as TNF-α, IL-6, and IL-12p70 (Fig. S4A). By using Huh7 cells harboring HCV subgenomic replicons (HCV-N, genotype 1b), we confirmed that the supernatants from poly IC-stimulated BDCA3$^+$ DCs suppressed HCV replication in an IL-28B concentration-dependent manner (Fig. S4B). Therefore, poly IC-stimulated BDCA3$^+$ DCs are capable of producing biologically active substances suppressing HCV replication, some part of which may be mediated by IFN-λs.

BDCA3$^+$ DCs Produce IL-28B upon HCVcc or HCV/JFH-1-Transfected Huh7.5.1 Cells. We stimulated freshly isolated BDCA3$^+$ DCs, pDCs and mDCs with infectious viruses, such as HCVcc, Japanese encephalitis virus (JEV), and herpes simplex virus (HSV). In preliminary experiments, we confirmed that HCVcc stimulated BDCA3$^+$ DCs to release IL-28B in a dose-dependent manner (Fig. S5). BDCA3$^+$ DCs

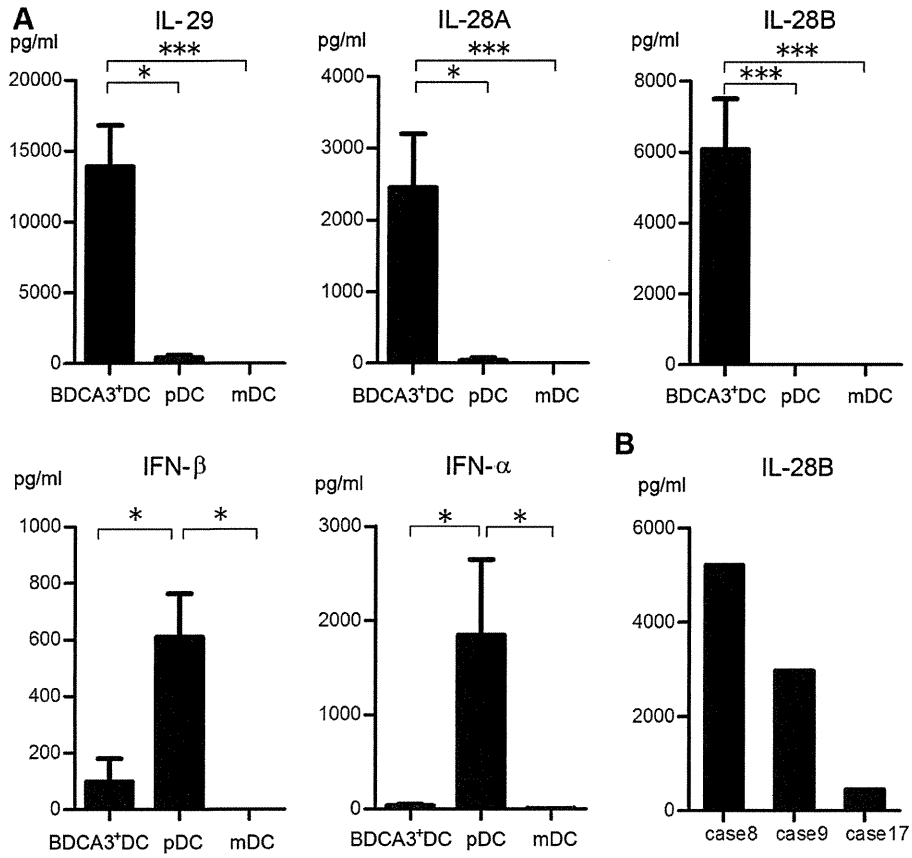

Fig. 3. BDCA3$^+$ DCs recovered from peripheral blood or intrahepatic lymphocytes produce large amounts of IL-29/IFN-λ1, IL-28A/IFN-λ2, and IL-28B/IFN-λ3 in response to poly IC. (A) BDCA3$^+$ DCs and mDCs were cultured at 2.5×10^4 cells with 25 mg/mL poly IC, and pDCs were with 5 mM CPG for 24 hours. The supernatants were examined for IL-29, IL-28A, IL-28B, IFN-β and IFN-α. Results are shown as mean $\pm$ SEM from 15 experiments. $^*P < 0.05$; $^{***}P < 0.0005$ by Kruskal-Wallis test. (B) For the IL-28B production, BDCA3$^+$ DCs in intrahepatic lymphocytes were cultured at 2.5×10^4 cells with 25 mg/mL poly IC for 24 hours. The samples of cases 8 and 9 were obtained from patients with non-B, non-C liver disease and that of case 17 was from an HCV-infected patient (Supporting Table 1).

produced a large amount of IL-28B upon exposure to HCVcc and released a lower amount of IFN-α upon HCVcc or HSV (Fig. 4A). In contrast, pDCs produced a large amount of IFN-α in response to HCVcc and HSV and a much lower level of IL-28B upon HCVcc (Fig. S6). In mDCs, IL-28B and IFN-α were not detectable with any of these viruses (data not shown).

BDCA3$^+$ DCs produced significantly higher levels of IL-28B than the other DCs upon HCVcc stimulation (Fig. 4B). By contrast, HCVcc-stimulated pDCs released significantly larger amounts of IFN-β and IFN-α than the other subsets (Fig. 4B). Liver BDCA3$^+$ DCs were capable of producing IL-28B in response to HCVcc (Fig. 4C). These results show that, upon HCVcc stimulation, BDCA3$^+$ DCs produce more IFN-λs and pDCs release more IFN-β and IFN-α than the other DC subsets, respectively. Taking a clinical impact of IL-28B genotypes on HCV eradication into consideration, we focused on IL-28B/IFN-λ3 as a representative for IFN-λs in the following experiments.

In a coculture with JFH-1-infected Huh7.5.1 cells, BDCA3$^+$ DCs profoundly released IL-29, IL-28A, and IL-28B (Fig. 4D, the results of IL-29 and IL-28A, not shown), whereas BDCA3$^+$ DCs failed to respond to Huh7.5.1 cells lacking HCV/JFH-1, showing that IL-28B production from BDCA3$^+$ DCs is dependent on HCV genome (Fig. 4D). In the absence of BDCA3$^+$ DCs, IL-28B is undetectable in the supernatant from JFH-1-infected Huh7.5.1 cells, demonstrating that BDCA3$^+$ DCs, not HCV-replicating Huh7.5.1 cells, produce detectable amount of IL-28B (Fig. 4D). In the coculture, BDCA3$^+$ DCs comparably released IL-28B either in the presence or the absence of transwells, suggesting that cell-to-cell contact between DCs and Huh7.5.1 cells is dispensable for IL-28B response (Fig. 4E). In parallel with the quantity of IL-28B in the coculture, ISG15 was significantly induced only in JFH-1-infected Huh7.5.1 cells cocultured with BDCA3$^+$ DCs (Fig. 4F). A strong induction was observed with other ISGs in JFH-1-infected Huh7.5.1 in the presence of BDCA3$^+$ DCs, such as IFIT1, MxA, RSD2, IP-10, and USP18 (Fig. S7). The results clearly show that BDCA3$^+$ DCs are capable of producing large amounts of IFN-λs in response to cellular or cell-free HCV, thereby inducing various ISGs in bystander liver cells.

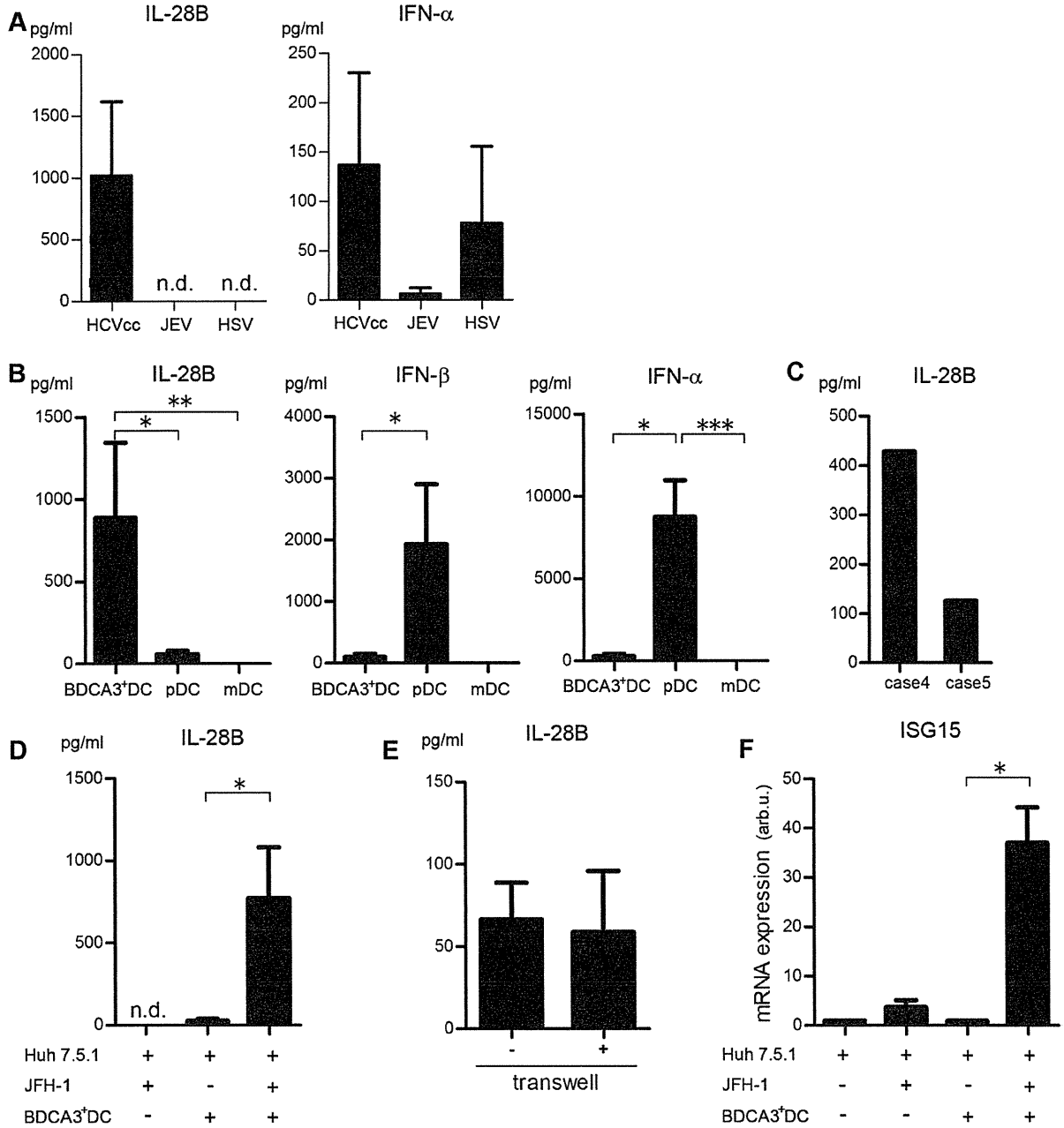

Fig. 4. BDCA3$^+$ DCs produce IL-29, IL-28A, and IL-28B upon cell-cultured HCV or HCV/JFH-1-transfected Huh7.5.1 cells, thereby inducing ISG. (A) BDCA3$^+$ DCs were cultured at 2.5 $\times$ 10^4 cells for 24 hours with HCVcc, JEV, or HSV at a multiplicity of infection (MOI) of 10. Results are shown as mean $\pm$ SEM from six experiments. n.d.; not detected. (B) BDCA3$^+$ DCs, pDCs, and mDCs were cultured at 2.5 $\times$ 10^4 cells for 24 hours with HCVcc at an MOI of 10. The results are shown as mean $\pm$ SEM from 11 experiments. *$P < 0.05$; **$P < 0.0005$; ***$P < 0.0005$ by Kruskal-Wallis test. (C) BDCA3$^+$ DCs recovered from intrahepatic lymphocytes were cultured at 2.5 $\times$ 10^4 cells for 24 hours with HCVcc at an MOI of 10. Both of the samples (cases 4 and 5) were obtained from patients with non-B, non-C liver disease. (D,E) BDCA3$^+$ DCs were cocultured at 2.5 $\times$ 10^4 cells with JFH-1-transfected (MOI = 2) or -untransfected Huh7.5.1 cells for 24 hours. The supernatants of JFH-1-transfected Huh7.5.1.cells without BDCA3$^+$ DCs were also examined. In some experiments of the coculture with JFH-1-transfected Huh7.5.1 cells and BDCA3$^+$ DCs, transwells were inserted into the wells (E). Results are shown as mean $\pm$ SEM from five experiments. *$P < 0.05$ by paired t test. (F) BDCA3$^+$ DCs were cocultured at 2.5 $\times$ 10^4 cells with JFH-1-transfected Huh7.5.1 cells (MOI = 2) or -untransfected Huh7.5.1 cells for 24 hours. The Huh7.5.1.cells were harvested and subjected to real-time RT-PCR analyses for ISG15 expression. The results are shown as mean $\pm$ SEM from five experiments. *$P < 0.05$ by paired t test. HCVcc, cell-cultured HCV; JEV, Japanese encephalitis virus; HSV, herpes simplex virus.

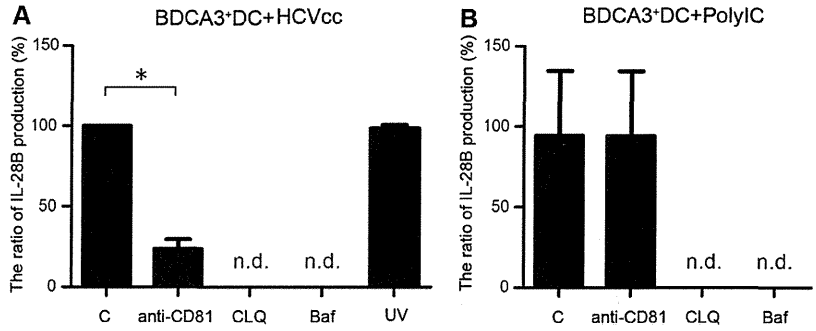

Fig. 5. The CD81 and endosome acidification is involved in the production of IL-28B from HCV-stimulated BDCA3$^+$ DCs, but HCV replication is not necessary. (A,B) BDCA3$^+$ DCs were cultured at 2.5 $\times$ 10^4 cells with HCVcc at an MOI of 10 (A) or poly IC (25 μg/mL) (B). In some experiments, UV-irradiated HCVcc was used at the same MOI, and BDCA3$^+$ DCs were treated with anti-CD81Ab (5 mg/mL), chloroquine (10 mM), or bafilomycin A1 (25 nM). The results are expressed as ratios of IL-28B quantity with or without the treatments. They are shown as mean $\pm$ SEM from five experiments. *$P < 0.05$ by paired t test. C, control; CLQ, treatment with chloroquine; Baf, treatment with bafilomycin A1; UV, ultraviolet-irradiated HCVcc; n.d., not detected.

CD81 and Endosome Acidification Are Involved in IL-28B Production from HCV-Stimulated BDCA3$^+$ DCs, but HCV Replication Is Not Involved. It is not known whether HCV entry and subsequent replication in DCs is involved or not in IFN response.[18,19] To test this, BDCA3$^+$ DCs were inoculated with UV-irradiated, replication-defective HCVcc. We confirmed that UV exposure under the current conditions is sufficient to negate HCVcc replication in Huh7.5.1 cells, as demonstrated by the lack of expression of NS5A after inoculation (data not shown). BDCA3$^+$ DCs produced comparable levels of IL-28B with UV-treated HCVcc, indicating that active HCV replication is not necessary for IL-28B production (Fig. 5A).

We next examined whether or not the association of HCVcc with BDCA3$^+$ DCs by CD81 is required for IL-28B production. It has been reported that the E2 region of HCV structural protein is associated with CD81 on cells when HCV enters susceptible cells.[13,20] We confirmed that all DC subsets express CD81, the degree of which was most significant on BDCA3$^+$ DCs (Fig. 1B, Fig. S1). Masking of CD81 with Ab significantly impaired IL-28B production from HCVcc-stimulated BDCA3$^+$ DCs in a dose-dependent manner (Fig. 5A, Fig. S8), suggesting that HCV-E2 and CD81 interaction is involved in the induction. The treatment of poly IC-stimulated BDCA3$^+$ DCs with anti-CD81 Ab failed to suppress IL-28B production (Fig. 5B).

HCV enters the target cells, which is followed by fusion steps within acidic endosome compartments. Chloroquine and bafilomycin A1 are well-known and broadly used inhibitors of endosome TLRs, which are reported to be capable of blocking TLR3 response in human monocyte-derived DC.[21,22] In our study, the treatment of BDCA3$^+$ DCs with chloroquine, bafilomycin A1, or NH4Cl significantly suppressed their IL-28B production either in response to HCVcc or poly IC (Fig. 5A,B, NH4Cl, data not shown). These results suggest that the endosome acidification is involved in HCVcc- or poly IC-stimulated BDCA3$^+$ DCs to produce IL-28B. The similar results were obtained with HCVcc-stimulated pDCs for the production of IL-28B (Fig. S9). We validated that such concentration of chloroquine (10 mM) and bafilomycin A1 (25 nM) did not reduce the viability of BDCA3$^+$ DCs (Fig. S10).

BDCA3$^+$ DCs Produce IL-28B in Response to HCVcc by a TIR-Domain-Containing Adapter-Inducing Interferon-β (TRIF)-Dependent Mechanism. TRIF/TICAM-1, a TIR domain-containing adaptor, is known to be essential for the TLR3-mediated pathway.[23] In order to elucidate whether TLR3-dependent pathway is involved or not in IL-28B response of BDCA3$^+$ DCs, we added the cell-permeable TRIF-specific inhibitory peptide (Invivogen) or the control peptide to poly IC- or HCVcc-stimulated BDCA3$^+$ DCs. Of particular interest, the TRIF-specific inhibitor peptide, but not the control one, significantly suppressed IL-28B production from poly IC- or HCVcc-stimulated BDCA3$^+$ DCs (Fig. 6A,B). In clear contrast, the TRIF-specific inhibitor failed to suppress IL-28B from HCVcc-stimulated pDCs (Fig. 6C), suggesting that pDCs recognize HCVcc in an endosome-dependent but TRIF-independent pathway. These results show that BDCA3$^+$ DCs may recognize HCVcc by way of the TRIF-dependent pathway to produce IL-28B.

BDCA3$^+$ DCs in Subjects with IL-28B Major Genotype Produce More IL-28B in Response to HCV than Those with IL-28B Minor Type. In order to compare the ability of BDCA3$^+$ DCs to release IL-28B in healthy subjects between IL28B major (rs8099917, TT)

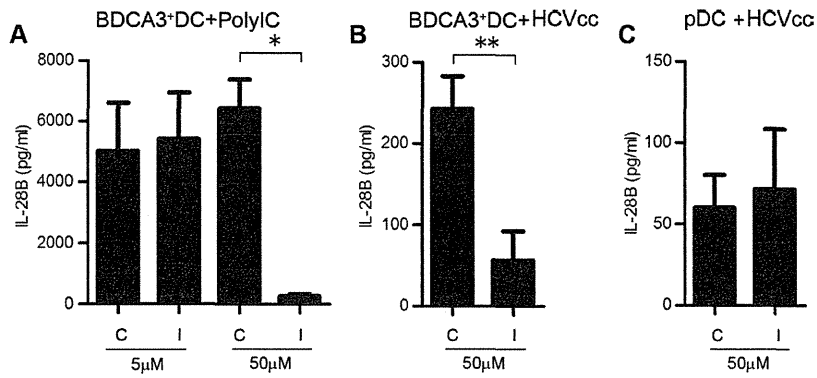

Fig. 6. BDCA3$^+$ DCs produce IL-28B upon HCVcc stimulation in a TRIF-dependent mechanism. BDCA3$^+$ DCs or pDCs had been treated with 5 or 50 mM TRIF inhibitory peptide or control peptide for 2 hours. Subsequently, BDCA3$^+$ DCs were stimulated with Poly IC (25 μg/mL) or HCVcc (MOI = 10), and pDCs were stimulated with HCVcc (MOI = 10), respectively. IL-28B was quantified by ELISA. They are shown as mean ± SEM from five experiments. *$P < 0.05$ by paired t test. C, TRIF control peptide; I, TRIF inhibitory peptide.

and minor hetero (TG) genotypes, we stimulated BDCA3$^+$ DCs of the identical subjects with poly IC (25 mg/mL, 2.5 mg/mL, 0.25 mg/mL), HCVcc or JFH-1-infected Huh 7.5.1, and subjected them to ELISA. The levels of IL-28B production by poly IC-stimulated BDCA3$^+$ DCs were comparable between subjects with IL-28B major and minor type (Fig. 7A). Similar results were obtained with the lesser concentrations of poly IC (Fig. S11). Of particular interest, in response to HCVcc or JFH-1 Huh7.5.1 cells, the levels of IL-28B from BDCA3$^+$ DCs were significantly higher in subjects with IL-28B major than those with minor type (Fig. 7B,C, S12).

Discussion

In this study we demonstrated that human BDCA3$^+$ DCs (1) are present at an extremely low frequency in PBMC but are accumulated in the liver; (2) are capable of producing IL-29/IFN-λ1, IL-28A/IFN-λ2, and IL-28B/IFN-λ3 robustly in response to HCV; (3) recognize HCV by a CD81-, endosome acidification and TRIF-dependent mechanism; and (4) produce larger amounts of IFN-λs upon HCV stimulation in subjects with IL-28B major genotype (rs8099917, TT). These characteristics of BDCA3$^+$ DCs are quite unique in comparison with other DC repertoires in the settings of HCV infection.

At the steady state, the frequency of DCs in the periphery is relatively lower than that of the other immune cells. However, under disease conditions or physiological stress, activated DCs dynamically migrate to the site where they are required to be functional. However, it remains obscure whether functional BDCA3$^+$ DCs exist or not in the liver. We identified BDCA3$^+$CLEC9A$^+$ cells in the liver tissue (Fig. 1D). In a paired frequency analysis of BDCA3$^+$ DCs between in PBMCs and in IHLs, the cells are more abundant in the liver. The phenotypes of liver BDCA3$^+$ DCs were more mature than the PBMC counterparts. In support of our observations, a recent publication showed that CD141$^+$ (BDCA3$^+$) DCs are accumulated and more mature in the liver, the trend of which is more in HCV-infected liver.[24] We confirmed that liver BDCA3$^+$ DCs are functional, capable of releasing IFN-λs in response to poly IC or HCVcc.

BDCA3$^+$ DCs were able to produce large amounts of IFN-λs but much less IFN-β or IFN-α upon TLR3 stimulation. In contrast, in response to TLR9 agonist,

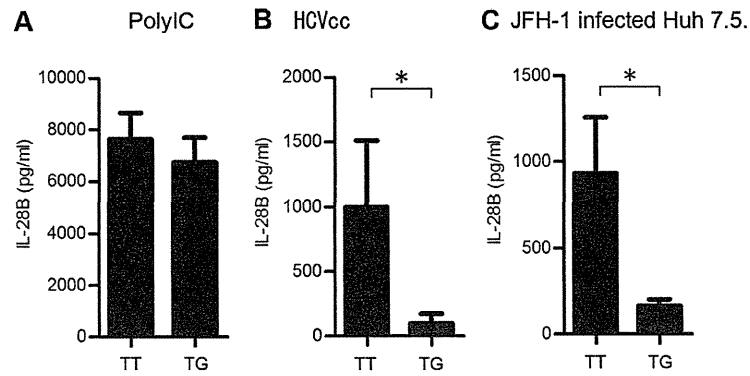

Fig. 7. In response to HCVcc, BDCA3$^+$ DCs of healthy donors with IL-28B major genotype (rs8099917, TT) produced more IL-28B than those with minor type (TG). BDCA3$^+$ DCs of healthy donors with IL-28B TT (rs8099917) or TG genotype were cultured at 2.5 × 10^4 cells with 25 mg/mL poly IC (A), with HCVcc at an MOI of 10 (B), or with JFH-1-infected Huh 7.5.1 cells (C) for 24 hours. The supernatants were subjected to IL-28B ELISA. The same healthy donors were examined for distinct stimuli. The results are the mean ± SEM from 15 donors with TT and 8 with TG, respectively. *$P < 0.05$ by Mann-Whitney U test.

pDCs released large amounts of IFN-β and IFN-α but much less IFN-λs. Such distinctive patterns of IFN response between BDCA3$^+$ DCs and pDCs are of particular interest. It has been reported that interferon regulatory factor (IRF)-3, IRF-7, or nuclear factor kappa B (NF-κB) are involved in IFN-β and IFN-λ1, while IRF-7 and NF-κB are involved in IFN-α and IFN-λ2/λ3.[5] Presumably, the stimuli with TLR3/retinoic acid-inducible gene-I (RIG-I) (poly IC) or TLR9 agonist (CpG-DNA) in DCs are destined to activate these transcription factors, resulting in the induction of both types of IFN at comparable levels. However, the results of the present study did not agree with such overlapping transcription factors for IFN-λs, IFN-β, and IFN-α. Two possible explanations exist for different levels of IFN-λs and IFN-α production by BDCA3$^+$ DCs and pDCs. First, the transcription factors required for full activation of IFN genes may differ according to the difference of DC subsets. The second possibility is that since type III IFN genes have multiple exons, they are potentially regulated by post-transcriptional mechanisms. Thus, it is possible that such genetic and/or posttranscriptional regulation is distinctively executed between BDCA3$^+$ DCs and pDCs. Comprehensive analysis of gene profiles downstream of TLRs or RIG-I in BDCA3$^+$ DCs should offer some information on this important issue.

BDCA3$^+$ DCs were found to be more sensitive to HCVcc than JEV or HSV in IL-28B/IFN-λ3 production. Such different strengths of IL-28B in BDCA3$^+$ DCs depending on the virus suggest that different receptors are involved in virus recognition. Again, the question arises of why BDCA3$^+$ DCs produce large amounts of IFN-λs compared to the amounts produced by pDCs in response to HCVcc. Considering that IRF-7 and NF-κB are involved in the transcription of the IL-28B gene, it is possible that BDCA3$^+$ DCs successfully activate both transcription factors upon HCVcc for maximizing IL-28B, whereas pDCs fail to do so. In support for this possibility, in pDCs it is reported that NF-κB is not properly activated upon HCVcc or hepatoma cell-derived HCV stimulations.[25]

In the present study we demonstrated that HCV entry into BDCA3$^+$ DCs through CD81 and subsequent endosome acidification are critically involved in IL-28B responses. Involvement of TRIF-dependent pathways in IL-28B production was shown by the significant inhibition of IL-28B with TRIF inhibitor. Nevertheless, active HCV replication in the cells is not required. Based on our data, we considered that BDCA3$^+$ DCs recognize HCV genome mainly by an endosome and TRIF-dependent mechanism. Although the results with UV-irradiated HCVcc, anti-CD81 blocking Ab, and chloroquine were quite similar, the TRIF-specific inhibitor failed to suppress IL-28B from pDCs (Fig. 6, Fig. S9).

In the coculture with JFH-transfected Huh7.5.1 cells, BDCA3$^+$ DCs presumably receive some signals for IL-28B production by way of cell-to-cell dependent and independent mechanisms. In the present study, most of the stimuli to BDCA3$^+$ DCs for IL-28B production may be the released HCVcc from Huh7.5.1 cells, judging from the inability of suppression with transwells. However, a contribution of contact-dependent mechanisms cannot be excluded in the coculture experiments. HCV genome is transmissible from infected hepatocytes to uninfected ones through tight junction molecules, such as claudin-1 and occuludin. Further investigation is needed to clarify whether such cell-to-cell transmission of viral genome is operated or not in BDCA3$^+$ DCs.

The relationship between IL-28B expression and the induction of ISGs has been drawing much research attention. In primary human hepatocytes, it is reported that HCV primarily induces IFN-λ, instead of type-I IFNs, subsequently enhancing ISG expression.[7] Of particular interest is that the level of hepatic IFN-λs is closely correlated with the strength of ISG response.[26] These reports strongly suggest that hepatic IFN-λs are a crucial driver of ISG induction and subsequent HCV eradication. Besides, it is likely that BDCA3$^+$ DCs, as a bystander IFN-λ producer in the liver, have a significant impact on hepatic ISG induction. In support of this possibility, we demonstrated in this study that BDCA3$^+$ DCs are capable of producing large amounts of IFN-λs in response to HCV, thereby inducing ISGs in the coexisting liver cells.

Controversial results have been reported regarding the relationship between IL28B genotypes and the levels of IL-28 expression. Nevertheless, in chronic hepatitis C patients with IL-28B major genotype, the IL-28 transcripts in PBMCs are reported to be higher than those with minor genotype.[2] In this study, by focusing on a prominent IFN-λ producer (BDCA3$^+$ DCs) and using the assay specific for IL-28B, we showed that the subjects with IL-28B major genotype could respond to HCV by releasing more IL-28B. Of interest, such a superior capacity of BDCA3$^+$ DCs was observed only in response to HCV but not to poly IC. Since the pathways downstream of TLR3-TRIF leading to IL-28B in BDCA3$^+$ DCs should be the same, either HCV or poly IC stimulation, two plausible explanations exist for such a distinct IL-28B response. First, it is possible that distinct epigenetic regulation may be

involved in IL-28B gene according to the IL-28B genotypes. Recently, in influenza virus infection, it is reported that micro-RNA29 and DNA methyltransferase are involved in the cyclooxygenase-2-mediated enhancement of IL-29/IFN-λ1 production.[27] This report supports the possibility that similar epigenetic machineries could be operated as well in HCV-induced IFN-λs production. Second, it is plausible that the efficiency of the stimulation of TLR3-TRIF may be different between the IL-28B genotypes. Since HCV reaches endosome in BDCA3$^+$ DCs by way of the CD81-mediated entry and subsequent endocytosis pathways, the efficiencies of HCV handling and enzyme reactions in endosome may be influential in the subsequent TLR3-TRIF-dependent responses. Certain unknown factors regulating such process may be linked to the IL-28B genotypes. For a comprehensive understanding of the biological importance of IL-28B in HCV infection, such confounding factors, if they exist, need to be explored.

In conclusion, human BDCA3$^+$ DCs, having a tendency to accumulate in the liver, recognize HCV and produce large amounts of IFN-λs. An enhanced IL-28B/IFN-λ3 response of BDCA3$^+$ DCs to HCV in subjects with IL-28B major genotype suggests that BDCA3$^+$ DCs are one of the key players in anti-HCV innate immunity. An exploration of the molecular mechanisms of potent and specialized capacity of BDCA3$^+$ DCs as IFN-λ producer could provide useful information on the development of a natural adjuvant against HCV infection.

References

1. Suppiah V, Moldovan M, Ahlenstiel G, Berg T, Weltman M, Abate ML, et al. IL28B is associated with response to chronic hepatitis C interferon-alpha and ribavirin therapy. Nat Genet 2009;41:1100-1104.
2. Tanaka Y, Nishida N, Sugiyama M, Kurosaki M, Matsuura K, Sakamoto N, et al. Genome-wide association of IL28B with response to pegylated interferon-alpha and ribavirin therapy for chronic hepatitis C. Nat Genet 2009;41:1105-1109.
3. Ge D, Fellay J, Thompson AJ, Simon JS, Shianna KV, Urban TJ, et al. Genetic variation in IL28B predicts hepatitis C treatment-induced viral clearance. Nature 2009;461:399-401.
4. Thomas DL, Thio CL, Martin MP, Qi Y, Ge D, O'Huigin C, et al. Genetic variation in IL28B and spontaneous clearance of hepatitis C virus. Nature 2009;461:798-801.
5. Kotenko SV. IFN-lambdas. Curr Opin Immunol 2011;23:583-590.
6. Urban TJ, Thompson AJ, Bradrick SS, Fellay J, Schuppan D, Cronin KD, et al. IL28B genotype is associated with differential expression of intrahepatic interferon-stimulated genes in patients with chronic hepatitis C. Hepatology 2010;52:1888-1896.
7. Park H, Serti E, Eke O, Muchmore B, Prokunina-Olsson L, Capone S, et al. IL-29 is the dominant type III interferon produced by hepatocytes during acute hepatitis C virus infection. Hepatology 2012;56:2060-2070.
8. Medzhitov R. Recognition of microorganisms and activation of the immune response. Nature 2007;449:819-826.
9. Liu YJ. Dendritic cell subsets and lineages, and their functions in innate and adaptive immunity. Cell 2001;106:259-262.
10. Poulin LF, Salio M, Griessinger E, Anjos-Afonso F, Craciun L, Chen JL, et al. Characterization of human DNGR-1+ BDCA3+ leukocytes as putative equivalents of mouse CD8alpha+ dendritic cells. J Exp Med 2010;207:1261-1271.
11. Lauterbach H, Bathke B, Gilles S, Traidl-Hoffmann C, Luber CA, Fejer G, et al. Mouse CD8alpha+ DCs and human BDCA3+ DCs are major producers of IFN-lambda in response to poly IC. J Exp Med 2010;207:2703-2717.
12. Wakita T, Pietschmann T, Kato T, Date T, Miyamoto M, Zhao Z, et al. Production of infectious hepatitis C virus in tissue culture from a cloned viral genome. Nat Med 2005;11:791-796.
13. Lindenbach BD, Evans MJ, Syder AJ, Wolk B, Tellinghuisen TL, Liu CC, et al. Complete replication of hepatitis C virus in cell culture. Science 2005;309:623-626.
14. Mori Y, Okabayashi T, Yamashita T, Zhao Z, Wakita T, Yasui K, et al. Nuclear localization of Japanese encephalitis virus core protein enhances viral replication. J Virol 2005;79:3448-3458.
15. Sugiyama M, Kimura T, Naito S, Mukaide M, Shinauchi T, Ueno M, et al. Development of interferon lambda 3 specific quantification assay for its mRNA and serum/plasma specimens. Hepatol Res 2012;42:1089-1099.
16. Schreibelt G, Klinkenberg LJ, Cruz LJ, Tacken PJ, Tel J, Kreutz M, et al. The C type lectin receptor CLEC9A mediates antigen uptake and (cross-)presentation by human blood BDCA3+ myeloid dendritic cells. Blood 2012;119:2284-2292.
17. Jongbloed SL, Kassianos AJ, McDonald KJ, Clark GJ, Ju X, Angel CE, et al. Human CD141+ (BDCA-3)+ dendritic cells (DCs) represent a unique myeloid DC subset that cross-presents necrotic cell antigens. J Exp Med 2010;207:1247-1260.
18. Marukian S, Jones CT, Andrus L, Evans MJ, Ritola KD, Charles ED, et al. Cell culture-produced hepatitis C virus does not infect peripheral blood mononuclear cells. Hepatology 2008;48:1843-1850.
19. Liang H, Russell RS, Yonkers NL, McDonald D, Rodriguez B, Harding CV, et al. Differential effects of hepatitis C virus JFH1 on human myeloid and plasmacytoid dendritic cells. J Virol 2009;83:5693-5707.
20. Zhang J, Randall G, Higginbottom A, Monk P, Rice CM, McKeating JA. CD81 is required for hepatitis C virus glycoprotein-mediated viral infection. J Virol 2004;78:1448-1455.
21. Blanchard E, Belouzard S, Goueslain L, Wakita T, Dubuisson J, Wychowski C, et al. Hepatitis C virus entry depends on clathrin-mediated endocytosis. J Virol 2006;80:6964-6972.
22. de Bouteiller O, Merck E, Hasan UA, Hubac S, Benguigui B, Trinchieri G, et al. Recognition of double-stranded RNA by human toll-like receptor 3 and downstream receptor signaling requires multimerization and an acidic pH. J Biol Chem 2005;280:38133-38145.
23. Takeda K, Akira S. TLR signaling pathways. Semin Immunol 2004;16:3-9.
24. Velazquez VM, Hon H, Ibegbu C, Knechtle SJ, Kirk AD, Grakoui A. Hepatic enrichment and activation of myeloid dendritic cells during chronic hepatitis C virus infection. Hepatology 2012;56:2071-2081.
25. Dental C, Florentin J, Aouar B, Gondois-Rey F, Durantel D, Baumert TF, et al. Hepatitis C virus fails to activate NF-kappaB signaling in plasmacytoid dendritic cells. J Virol 2012;86:1090-1096.
26. Thomas E, Gonzalez VD, Li Q, Modi AA, Chen W, Noureddin M, et al. HCV infection induces a unique hepatic innate immune response associated with robust production of type III interferons. Gastroenterology 2012;142:978-988.
27. Fang J, Hao Q, Liu L, Li Y, Wu J, Huo X, Zhu Y. Epigenetic changes mediated by microRNA miR29 activate cyclooxygenase 2 and lambda-1 interferon production during viral infection. J Virol 2012;86:1010-1020.

Hepatology Research

Hepatology Research 2013; 43: 1284–1294 doi: 10.1111/hepr.12095

Original Article

Clinical usefulness of non-protein respiratory quotient measurement in non-alcoholic fatty liver disease

Keiko Korenaga,[1] Masaaki Korenaga,[1] Fusako Teramoto,[3] Toshiko Suzuki,[4] Sohji Nishina,[1] Kyo Sasaki,[1] Yoshihiro Nakashima,[1] Yasuyuki Tomiyama,[1] Naoko Yoshioka,[1] Yuichi Hara,[1] Takuya Moriya[2] and Keisuke Hino[1]

Departments of [1]Hepatology and Pancreatology and [2]Pathology, Kawasaki Medical School, [3]Department of Clinical Nutrition, Kawasaki University of Medical Welfare, and [4]Department of Nutrition, Kawasaki Medical School Hospital, Kurashiki, Okayama, Japan

Aim: Little is known about the effects of non-alcoholic fatty liver disease (NAFLD) on energy metabolism, although this disease is associated with metabolic syndrome. We measured non-protein respiratory quotient (npRQ) using indirect calorimetry, which reflects glucose oxidation, and compared this value with histological disease severity in NAFLD patients.

Methods: Subjects were 32 patients who were diagnosed with NAFLD histopathologically. Subjects underwent body composition analysis and indirect calorimetry, and npRQ was calculated. An oral glucose tolerance test was performed, and plasma glucose area under the curve (AUC glucose) was calculated.

Results: There were no differences in body mass index, body fat percentage or visceral fat area among fibrosis stage groups. As fibrosis progressed, npRQ significantly decreased (stage 0, 0.895 ± 0.068; stage 1, 0.869 ± 0.067; stage 2, 0.808 ± 0.046; stage 3, 0.798 ± 0.026; $P < 0.005$). Glucose intolerance worsened and insulin resistance increased with fibrosis stage. npRQ was negatively correlated with AUC glucose ($R = -0.6308$, $P < 0.001$), Homeostasis Model of Assessment – Insulin Resistance ($R = -0.5045$, $P < 0.005$), fasting glucose ($R = -0.4585$, $P < 0.01$) and insulin levels ($R = -0.4431$, $P < 0.05$), suggesting that decreased npRQ may reflect impaired glucose tolerance due to insulin resistance, which was associated with fibrosis progression. Estimation of fibrosis stage using npRQ was as accurate as several previously established scoring systems using receiver–operator curve analysis.

Conclusion: npRQ was significantly decreased in patients with advanced NAFLD. Our data suggest that measurement of npRQ is useful for the estimation of disease severity in NAFLD patients.

Key words: glucose intolerance, NAFLD, npRQ

INTRODUCTION

NON-ALCOHOLIC FATTY LIVER disease (NAFLD) is one of the most common chronic liver diseases. NAFLD is associated with metabolic syndrome and insulin resistance and often involves abnormal glucose and lipid metabolism.[1–6] Based on this, the NAFLD Asia–Pacific Working Party has recommended screening for metabolic syndrome and body composition in all NAFLD patients.[6] NAFLD treatment consists of diet and exercise interventions for weight loss,[4–6] and nutritional guidance and management are essential. As a part of a nutritional guidance and management program, our institution performs anthropometric measurement of NAFLD patients using a body composition analyzer, evaluation of glucose metabolism using a 75-g oral glucose tolerance test (OGTT), and evaluation of energy metabolism using indirect calorimetry. These basic tests are performed in routine practice.

Indirect calorimetry is a method used in physiological testing and enables easy and non-invasive evaluation of energy metabolism in real time.[7] The non-protein respiratory quotient (npRQ) calculated from indirect calorimetry data represents the ratio of carbohydrate to fat oxidation, and its value is said to be an indicator of prognosis in liver cirrhosis.[8] In addition, although it has been reported that NAFLD disease progression is

Correspondence: Masaaki Korenaga, The Research Center for Hepatitis and Immunology, National Center for Global Health and Medicine at Kohonodai, 1-7-1 Kohnodai, Ichikawa, Chiba 272-8516, Japan. Email; makorena@coffee.ocn.ne.jp
Received 26 December 2012; revision 4 February 2013; accepted 11 February 2013.

associated with glucose intolerance[9–12] and visceral fat accumulation,[13] no previous study has examined the specific relationship between NAFLD pathology and these nutritional parameters.

One aim of the present study was to elucidate whether nutritional status, as estimated by indirect calorimetry, 75-g OGTT and body composition analysis, was related to NAFLD disease progression. The other aim was to elucidate whether these parameters were useful for prediction of the severity of disease.

METHODS

Patients

SUBJECTS WERE 32 patients diagnosed with NAFLD/non-alcoholic steatohepatitis (NASH) by biopsy between April 2009 and March 2011 at our institution. All patients had untreated impaired glucose tolerance (no drug treatment) and present and past alcohol consumption of 20 g or less per week. No patient had been treated with drugs, such as tamoxifen, that can induce NAFLD/NASH. Patients were excluded if they had liver cirrhosis with decreased npRQ accompanied by protein energy malnutrition (PEM).[8] Other exclusion criteria included a history of liver diseases such as primary biliary cirrhosis, autoimmune hepatitis, hepatitis B infection or hepatitis C infection. Hepatocellular carcinoma (HCC) was not detected in any patient.

The study protocol was approved by the institutional review board. Written informed consent was obtained from all patients before trial registration. For all patients, tests were performed in the hospital under resting, fasted conditions in the early morning.

Study design

All subjects were hospitalized for at least 2 days to undergo a liver biopsy. Indirect calorimetry and 75-g OGTT were performed before liver biopsy, as described below. Anthropometric measurements and laboratory analysis were carried out before the indirect calorimetry study. All subjects received nutritional guidance from dieticians and were prescribed medical nutrition therapy (energy 25–30 kcal/kg ideal bodyweight).

Physical examination and serum biochemistry

Anthropometric measurements (body mass index [BMI], body fat percentage, and visceral fat area [VFA]) were performed using a body composition analyzer (InBody 720; BIOSPACE, Tokyo, Japan). We previously determined VFA values using a body composition analyzer and performed abdominal computed tomography using Fat Scan software (E2 system, Osaka, Japan) in 27 NAFLD patients. There was a strong correlation between these two modalities ($n = 27$, $R = 0.9319$, $P < 0.0001$; unpubl. data). Venous blood samples were collected in the early morning after patients had fasted for 12 h. These samples were used for several biochemical tests.

NAFIC score,[14] NAFLD fibrosis score[15] and FIB-4 index[16] were calculated using previously reported formulas.

75-g OGTT

A 75-G OGTT was performed, and plasma glucose and immunoreactive insulin (IRI) were measured at 0, 30, 60, 90 and 120 min after glucose loading. Based on the classification of the Expert Committee on the Diagnosis and Classification of DM,[17] individuals were diagnosed with impaired fasting glucose (IFG) if they had fasting plasma glucose levels of 110 mg/dL or more, but less than 126 mg/dL, and if they had a plasma glucose level less than 140 mg/dL at 120 min after glucose loading. Individuals were diagnosed with impaired glucose tolerance (IGT) if they had plasma glucose levels of less than 110 mg/dL at 0 min after loading and exceeding 140 mg/dL at 120 min after loading. Individuals were diagnosed with diabetes mellitus (DM) if they had plasma glucose levels exceeding 200 mg/dL at 120 min after loading. Homeostasis Model of Assessment – Insulin Resistance (HOMA-IR) was calculated using the following formula:[18] HOMA-IR = fasting insulin (mU/mL) × plasma glucose (mg/dL) / 405. Plasma glucose area under the curve (AUC glucose) and IRI area under the curve (AUC IRI) were calculated using methods reported previously.[19]

Indirect calorimetry

Energy metabolism was measured by indirect calorimetry (Aero Monitor AE-300s; Minato Medical Science, Osaka, Japan). A previously reported method[19] was used to measure oxygen uptake and carbon dioxide exhalation under resting, fasted conditions in the early morning. Twenty-four-hour urine nitrogen levels were also measured. The resulting values were used to calculate npRQ and resting energy expenditure (REE). The basal metabolic rate (BMR) was calculated using the Harris–Benedict formula.[20]

Pathology

All samples were diagnosed by a pathologist who was not notified of subjects' clinical data or course. The

classification of Brunt *et al.*[21] was used for fibrosis staging, and disease activity was assessed using the NAFLD activity score (NAS).[22]

Statistical analyses

Statistical analysis was performed using SPSS ver. 20.0 software (SPSS, Chicago, IL, USA). Results were expressed as mean ±standard deviation or standard error of the mean. A χ^2-test was used for categorical variables. A Student's *t*-test or Mann–Whitney *U*-test was used to compare two groups. One-way ANOVA or Kruskal–Wallis analysis followed by a post-hoc test was used to compare multiple independent groups. Correlation was assessed using Spearman's correlation coefficient. Receiver-operator curves (ROC) were used to assess discrimination ability. Statistical significance was defined as $P < 0.05$.

RESULTS

Patients

THE CLINICAL AND biochemical characteristics of patients enrolled in the study are summarized in Table 1. The 32 subjects (24 male, eight female) had a mean age of 45.4 years (range, 27–75). BMI ranged 22.0–38.8 kg/m^2 and averaged 27.2 kg/m^2. Serum alanine aminotransferase (ALT) levels ranged 22–200 IU/L and averaged 95.6 IU/L. Histological findings are shown also in Table 1. Fibrosis stages were determined according to Brunt *et al.*'s classification,[21] and there were eight patients at stage 0, 10 patients at stage 1, seven patients at stage 2 and seven patients at stage 3. For NAS, there were six patients with scores of less than 3, 20 patients with scores of 3 or 4, and six patients with scores of 5 or more.

Anthropometric measurements

Body mass index, body fat percentage and VFA tended to increase as fibrosis progressed. However, there was no significant difference in these parameters among groups with different Brunt stages (Table 2).

75-g OGTT

Four patients (12.5%) had HbA1c levels of at least 6.1% or fasting glucose of at least 110 mg/dL and in whom impaired glucose tolerance was suspected before the 75-g OGTT. The 75-g OGTT did not reveal a normal glucose tolerance pattern in any patient, and all patients had impaired glucose metabolism. One patient (3.1%) had IFG, 16 patients (50.0%) had IGT and 15 patients (46.9%) had DM.

Table 1 Characteristics of the patient population ($n = 32$)

Variable	
Sex (male/female)	24/8
Age (years)	45.4 ± 12.2
BMI (kg/m^2)	27.2 ± 4.0
AST (IU/L)	65.6 ± 73.4
ALT (IU/L)	95.6 ± 62.7
γ-GT (IU/L)	91.3 ± 76.8
Total cholesterol (mg/dL)	206.7 ± 44.7
Triglyceride (mg/dL)	155.4 ± 85.2
NEFA (μEq/L)	552.1 ± 212.0
Albumin (g/dL)	4.4 ± 0.5
Prothrombin time (%)	104.6 ± 11.2
Platelet count (X 10^4/μL)	23.7 ± 6.2
P-III-P (U/mL)	0.64 ± 0.28
Type IV collagen 7S (ng/mL)	4.4 ± 2.2
Fasting glucose (mg/dL)	94.4 ± 15.6
75-g oral glucose tolerance test	
Normal/IFG/ IGT/DM	0/1/16/15
Histological assessment	
Stage (0/1/2/3)†	8/10/7/7
Grade (0/1/2/3)†	8/6/14/4
NAS (<3/ 3,4/ ≥5)	6/20/6

Results are expressed as mean ± standard deviation.
†Stage and grade on histological assessment were determined using Brunt's classification.[21]
ALT, alanine aminotransferase; AST, aspartate aminotransferase; BMI, body mass index; DM, diabetes mellitus; γ-GT, γ-glutamyl transferase; IFG, impaired fasting glucose; IGT, impaired glucose tolerance; NAFLD, non-alcoholic fatty liver disease; NAS, NAFLD activity score; NEFA, non-esterified fatty acid.

Fasting glucose, HbA1c and AUC glucose increased as fibrosis progressed, and glucose metabolism was significantly worsened with fibrosis progression (Table 2). The 75-g OGTT revealed a correlation between postprandial hyperglycemia and Brunt stage (Fig. 1a). There were significant differences among fibrosis stages in plasma glucose levels at 0, 30 and 120 min after loading ($P < 0.05$ using Kruskal–Wallis analysis).

In patients with fibrosis stages 1–3, fasting insulin levels were increased and HOMA-IR was elevated, indicating the presence of insulin resistance. This tendency was significantly more pronounced in more advanced fibrosis stages (Table 2). In the 75-g OGTT (Fig. 1b), insulin secretion was delayed and postprandial hyperinsulinemia was observed for all stages compared with healthy controls, as previously reported.[23] In particular, stage 3 patients had significantly greater hyperinsulinemia than patients at the other stages at 0, 90 and 120 min after loading ($P < 0.05$ using Kruskal–Wallis analysis).

Table 2 Clinical features and laboratory data of NAFLD/NASH patients determined using Brunt *et al.*'s classification[21]

Variable	Stage 0 ($n = 8$)	Stage 1 ($n = 10$)	Stage 2 ($n = 7$)	Stage 3 ($n = 7$)	*P*-value†
Sex (male/female)	5/3	8/2	5/2	6/1	0.7348
Age (years)	46.1 ± 11.4	40.3 ± 13.0	46.3 ± 11.9	50.8 ± 11.8	0.3713
BMI (kg/m^2)	25.1 ± 1.9	27.2 ± 5.9	27.6 ± 2.2	29.1 ± 3.1	0.2714
Percent body fat (%)	30.3 ± 6.8	28.7 ± 8.4	33.6 ± 6.7	33.2 ± 7.1	0.5082
VFA (cm^2)	116.7 ± 22.3	122.3 ± 47.5	141.4 ± 26.7	163.5 ± 46.8	0.1029
AST (IU/L)	29.8 ± 5.4	48.6 ± 22.6	78.7 ± 35.5	117.7 ± 142.3	<0.01
ALT (IU/L)	43.3 ± 26.7	91.5 ± 51.8	131.0 ± 43.2	125.7 ± 86.0	<0.05
γ-GT (IU/L)	74.4 ± 29.1	85.1 ± 73.9	75.7 ± 45.1	134.9 ± 127.6	0.5789
Total cholesterol (mg/dL)	200.6 ± 23.0	214.8 ± 59.5	200.9 ± 30.0	188.0 ± 52.1	0.5131
Triglyceride (mg/dL)	116.8 ± 6.5	181.9 ± 109.3	170.8 ± 87.2	145.1 ± 75.6	0.5364
NEFA (μEq/L)	494.0 ± 231.9	571.8 ± 285.0	619.2 ± 31.0	532.9 ± 171.4	0.8629
Type IV collagen 7S (ng/mL)	3.51 ± 0.71	3.46 ± 0.98	3.82 ± 0.54	6.94 ± 3.12	<0.05
Ferritin (ng/mL)	157.0 ± 45.9	225.1 ± 208.9	178.4 ± 67.9	474.4 ± 578.5	<0.05
Fasting glucose (mg/dL)	85.5 ± 8.69	88.6 ± 7.71	109.7 ± 21.5	110.4 ± 34.7	<0.05
Fasting insulin (μU/mL)	8.00 ± 3.62	11.3 ± 4.81	15.2 ± 10.8	26.1 ± 15.3	<0.005
HOMA-IR	1.70 ± 0.80	2.46 ± 1.19	4.11 ± 3.03	6.56 ± 2.78	<0.005
Hemoglobin A1c (%)	5.61 ± 0.55	5.41 ± 0.38	5.97 ± 0.89	6.74 ± 1.75	<0.05
75-g OGTT					
Normal/IFG/IGT/DM	0/0/6/2	0/1/6/3	0/0/4/3	0/0/0/7	
AUC glucose (mg·h/dL)	363.8 ± 64.9	406.4 ± 87.2	450.6 ± 39.0	497.1 ± 45.8	<0.005
AUC IRI (μU·h/mL)	247.4 ± 130.6	247.7 ± 99.1	238.54 ± 96.2	536.2 ± 305.1	<0.05
Indirect calorimetry					
npRQ	0.895 ± 0.068	0.869 ± 0.067	0.808 ± 0.046	0.798 ± 0.026	<0.005
REE/BMR	0.922 ± 0.091	0.922 ± 0.160	1.034 ± 0.069	1.021 ± 0.073	0.2495
NAFIC score[14]	0.125 ± 0.354	0.600 ± 0.699	0.857 ± 0.378	2.143 ± 0.900	<0.0005
NAFLD fibrosis score[15]	−2.77 ± 1.13	−2.55 ± 1.08	−2.06 ± 0.69	−0.73 ± 1.92	<0.05
FIB-4 index[16]	0.880 ± 0.331	0.952 ± 0.472	1.326 ± 0.674	2.564 ± 2.391	<0.05

Results are expressed as mean ± standard deviation.
†*P*-value for four-group comparisons.
Differences and correlations among the four groups were determined using one-way ANOVA or Kruskal–Wallis analysis followed by a post-hoc test.
ALT, alanine aminotransferase; AST, aspartate aminotransferase; AUC glucose, plasma glucose area under the curve; AUC IRI, immunoreactive insulin area under the curve; BMI, body mass index; BMR, basal metabolic rate; DM, diabetes mellitus; γ-GT, γ-glutamyl transferase; HOMA-IR, homeostasis model assessment of insulin resistance; IFG, impaired fasting glucose; IGT, impaired glucose tolerance; NEFA, non-esterified fatty acid; npRQ, non protein respiratory quotient; 75-g OGTT, 75-g oral glucose tolerance test; REE, resting energy expenditure; VFA, visceral fat area.

Indirect calorimetry

Non-protein respiratory quotient values determined using indirect calorimetry data significantly decreased as fibrosis progressed (Table 2, Fig. 2a). In addition, npRQ values significantly decreased as NAS increased (Fig. 2b). There was no relationship between npRQ and disease activity (Fig. 2c).

Resting energy expenditure and BMR predicted using the Harris–Benedict formula[20] did not differ among Brunt stages or NAS classifications (data not shown). The ratio of REE to BMR (REE/BMR) also did not differ among Brunt stages (Table 2) or NAS classifications (data not shown). In addition, this ratio was within the normal range ($0.9 < \text{REE/BMR} < 1.1$),[8] indicating that most subjects were in normal metabolic states, and not hyper- or hypometabolic states.

Blood biochemistry

There were significant differences among stages in AST, ALT, type IV collagen 7S and ferritin levels (Table 2). However, there were no significant differences among stages with respect to other parameters, including γ-glutamyl transferase (γ-GT), total cholesterol, triglyceride and non-esterified fatty acid (NEFA) (Table 2),

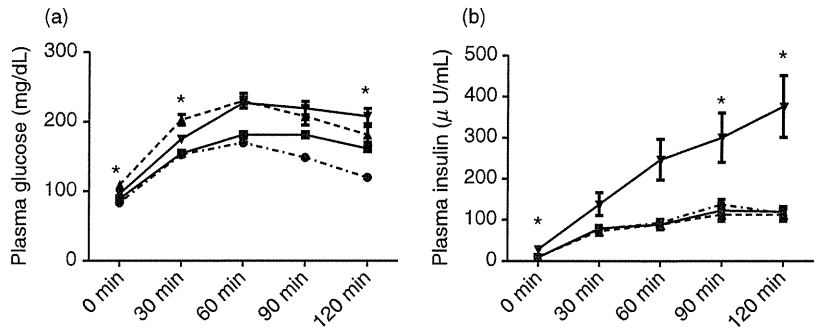

Figure 1 (a) Serum glucose levels during a 75-g oral glucose tolerance test in non-alcoholic fatty liver disease (NAFLD) patients. *There were significant differences among stages in plasma glucose levels at 0, 30 and 120 min ($P < 0.05$) after loading as determined by Kruskal–Wallis analysis. (b) Serum insulin levels during a 75-g oral glucose tolerance test in NAFLD patients. *There were significant differences among stages in plasma glucose levels at 0, 90 and 120 min ($P < 0.05$) after loading as determined by Kruskal–Wallis analysis. Results are expressed as mean ± standard error of the mean. ·-●-, Stage 0; —■—, stage 1; -▲-, stage 2; —▼—, stage 3.

AST/ALT ratio, hyaluronic acid, platelet count and prothrombin time (data not shown).

Comparison of patients with mild fibrosis (stages 0–1) and patients with more advanced fibrosis (stages 2–3)

To identify factors correlated with fibrosis in NAFLD patients, we divided subjects into two groups – those with mild fibrosis (stages 0–1) and those with more advanced fibrosis (stages 2–3) – and compared clinical features.

Patients with more advanced fibrosis had significantly higher values than patients with mild fibrosis for the following parameters: VFA, serum AST, ALT, P-III-P, type IV collagen 7S, fasting glucose, fasting insulin, HOMA-IR, HbA1c and AUC glucose (Table 3). Patients having more advanced fibrosis had significantly lower npRQ values than patients with mild fibrosis (Table 3). There were no significant differences between the two groups with respect to other parameters, including γ-GT, total cholesterol, triglyceride and NEFA (data not shown).

Correlation of npRQ with parameters of glucose and fat metabolism and body composition

We next compared npRQ to parameters of glucose and fat metabolism and body composition. There was a negative correlation between npRQ and AUC glucose ($R = -0.6308$, $P < 0.001$ using Spearman's correlation coefficient) (Fig. 3a). There was also a negative correla-

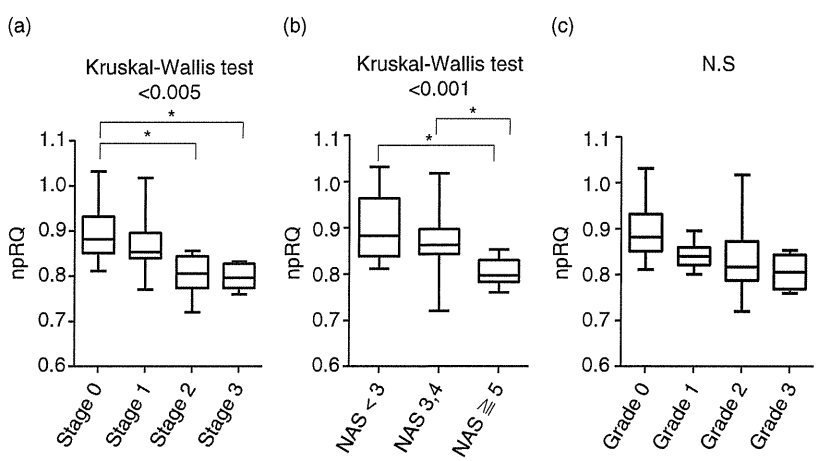

Figure 2 Non-protein respiratory quotient (npRQ) in non-alcoholic fatty liver disease (NAFLD) patients. (a) By stage. (b) By NAFLD activity score (NAS). (c) By grade. There was a significant difference in npRQ among (a) stages and (b) NAS. *Post-hoc test showed a significant difference ($P < 0.05$). N.S., not significant.

Table 3 Comparison of clinical features and laboratory data between stages 0–1 versus stages 2–3 in NAFLD/NASH patients

	Stages 0–1 ($n = 18$)	Stages 2–3 ($n = 14$)	*P*-value†
Sex (male/female)	13/5	11/3	0.6807
Age (years)	42.9 ± 12.35	48.6 ± 11.6	0.1947
BMI (kg/m^2)	26.3 ± 4.6	28.4 ± 2.8	0.1419
Percent body fat (%)	29.4 ± 7.6	33.4 ± 6.7	0.1398
VFA (cm^2)	119.7 ± 36.8	153.3 ± 39.0	<0.05
AST (IU/L)	40.2 ± 19.4	98.2 ± 101.7	<0.05
ALT (IU/L)	70.1 ± 48.2	128.4 ± 65.5	<0.01
P-III-P (U/mL)	0.53 ± 0.10	0.81 ± 0.38	<0.01
Type IV collagen 7S (ng/mL)	3.48 ± 0.84	5.64 ± 2.83	<0.005
Fasting glucose (mg/dL)	87.2 ± 8.1	104.3 ± 18.2	<0.005
Fasting insulin (μU/mL)	9.9 ± 4.5	21.3 ± 14.2	<0.005
HOMA-IR	2.1 ± 1.1	5.2 ± 3.1	<0.0005
Hemoglobin A1c (%)	5.5 ± 0.5	6.0 ± 0.7	<0.05
75-g OGTT			
Normal/IFG/IGT/DM	0/1/12/5	0/0/4/10	
AUC glucose (mg·h/dL)	379.4 ± 64.2	473.4 ± 49.4	<0.0005
AUC IRI (μU·h/mL)	254.2 ± 100.6	371.8 ± 261.6	0.1448
Indirect calorimetry			
npRQ	0.881 ± 0.067	0.803 ± 0.036	<0.0005

Results are expressed as mean ± SD.
†*P*-value for two comparisons.
Differences between two groups were determined using Student's *t*-test, Mann-Whitney's *U*-test, or chi-square test.
ALT, alanine aminotransferase; AST, aspartate aminotransferase; AUC glucose, blood glucose area under the curve; AUC IRI, immunoreactive insulin area under the curve; BMI, body mass index; DM, diabetes mellitus; γ-GT, γ-glutamyl transferase; HOMA-IR, Homeostasis Model of Assessment – Insulin Resistance; IFG, impaired fasting glucose; IGT, impaired glucose tolerance; NAFLD, non-alcoholic fatty liver disease; NASH, non-alcoholic steatohepatitis; npRQ, non-protein respiratory quotient; 75-g OGTT, 75-g oral glucose tolerance test; VFA, visceral fat area.

tion between npRQ and HOMA-IR ($R = -0.5045$, $P < 0.005$) (Fig. 3b). A weak negative correlation was found between npRQ and fasting glucose ($R = -0.4585$, $P < 0.01$) (Fig. 3c), fasting insulin ($R = -0.4431$, $P < 0.05$) (Fig. 3d), γ-GT ($R = -0.4428$, $P < 0.05$), plasma glucose levels 120 min after loading ($R = -0.3684$, $P < 0.05$) and IRI levels 120 min after loading in the OGTT ($R = -0.3772$, $P < 0.05$). No significant correlation was found between npRQ and AUC IRI ($R = -0.2992$, $P = 0.1021$), total cholesterol ($R = -0.2499$, $P = 0.1678$), triglyceride ($R = -0.0617$, $P = 0.7599$), NEFA ($R = -0.0629$ $P = 0.7367$), BMI ($R = -0.3165$, $P = 0.0776$), body fat percentage ($R = -0.1233$, $P = 0.5088$) or VFA ($R = -0.2308$, $P = 0.2199$). Based on these results, we speculated that low npRQ in NAFLD is associated with impaired glucose tolerance due to insulin resistance.

Comparison of npRQ to several parameters and previously established scoring systems

We calculated area under the ROC (AUROC) for npRQ and for several of the parameters shown in Table 2. We compared these AUROC to see if they could differentiate stage 3 from stages 0–2, stages 2–3 from stages 0–1, and stage 0 from stages 1–3. Table 4 summarizes these results. For differentiation of stages 3 from stages 0–2, the calculated AUROC was greatest for NAFIC score (0.9200), followed by HOMA-IR (0.9100), type IV collagen 7S (0.8820), AUC glucose and fasting insulin (0.8743), ferritin (0.8690) and npRQ (0.8343). For differentiation of stages 2–3 from stages 0–1, the AUROC for npRQ was greatest (0.8849), followed by HOMA-IR (0.8846), AUC glucose (0.8690), fasting glucose (0.8651), NAFIC score (0.8373) and fasting insulin (0.8234). For differentiation of stage 0 from stages 1–3, the AUROC for ALT was greatest (0.8568), followed by AST (0.8542), fasting insulin (0.8490), HOMA-IR and AUC glucose (both 0.8478), NAFIC score (0.8281) and npRQ (0.8203).

In each of the three comparisons of stages, AUROC for npRQ, HOMA-IR, AUC glucose, fasting insulin and NAFIC score were all over 0.8000 and showed relatively good results. To differentiate stage 3 from stages 0–2, the AUROC for type IV collagen 7S and ferritin were

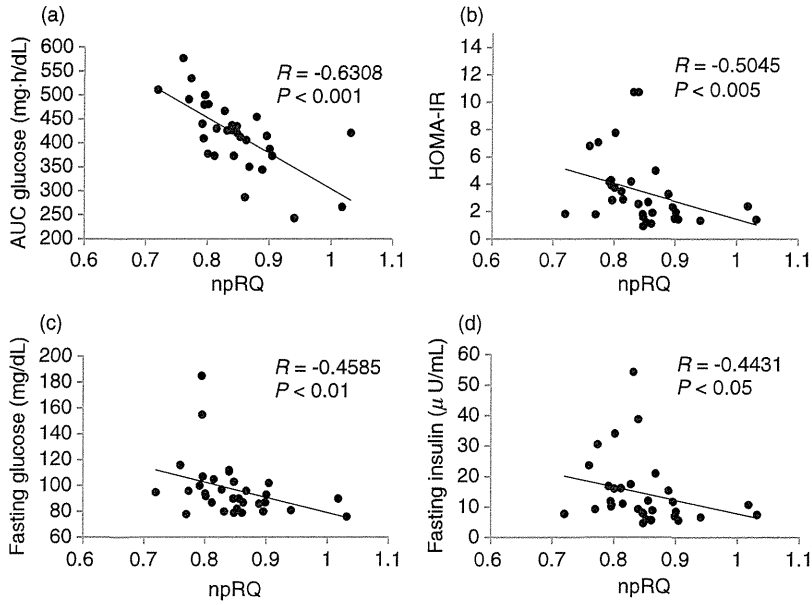

Figure 3 Correlation between non-protein respiratory quotient (npRQ) and other parameters ($n = 32$). (a) With area under the curve (AUC) glucose. (b) With Homeostasis Model of Assessment – Insulin Resistance. (c) With fasting glucose. (d) With fasting insulin.

Table 4 AUROC for npRQ, other biochemical parameters and scoring systems for NAFLD/NASH patients

Variable	AUROC Stage 0 vs. Stages 1–3	AUROC Stages 0–1 vs. Stages 2–3	AUROC Stages 0–2 vs. Stage 3
npRQ	0.8203	0.8849	0.8343
HOMA-IR	0.8478	0.8846	0.9100
AUC glucose	0.8478	0.8690	0.8743
AUC IRI	0.5924	0.6154	0.8133
Fasting glucose	0.7813	0.8651	0.7143
Fasting insulin	0.8490	0.8234	0.8743
Hemoglobin A1c	0.5617	0.7668	0.8080
Type IV collagen 7S	0.5893	0.7870	0.8820
NAFIC score[14]	0.8281	0.8373	0.9200
NAFLD fibrosis score[15]	0.6615	0.7460	0.8057
FIB-4 index[16]	0.6250	0.7222	0.7143
AST	0.8542	0.7976	0.6514
ALT	0.8568	0.7778	0.6343
Ferritin	0.5893	0.6912	0.8690

ALT, alanine aminotransferase; AST, aspartate aminotransferase; AUC glucose, plasma glucose area under the curve; AUC IRI, immunoreactive insulin area under the curve; AUROC, area under the receiver-operator curve; HOMA-IR, homeostasis model assessment of insulin resistance; NAFLD, non-alcoholic fatty liver disease; NASH, non-alcoholic steatohepatitis; npRQ, non-protein respiratory quotient.

high; however, AUROC for these parameters were not able to differentiate stage 0 from stages 1–3. This is due to the fact that these two parameters had elevated values in stage 3 and there was no significant difference from stage 0 to stage 2. The AUROC for NAFLD fibrosis score and FIB-4 index were lowest for differentiation of stage 0 from stages 1–3, and increased for differentiation of stages 2–3 from stages 0–1 and differentiation of stage 3 from stages 0–2. This result suggests that these two methods of scoring fibrosis had a relatively high degree of accuracy in distinguishing severe from mild or no fibrosis. AUROC for AST and ALT could be used to differentiate stage 0 from stages 1–3, but were not as accurate in differentiating stage 3 from stages 0–2.

DISCUSSION

NON-ALCOHOLIC FATTY LIVER disease comprises a wide spectrum of conditions ranging from simple steatosis to NASH, which can progress to cirrhosis and HCC. Patients with advanced liver fibrosis are considered to be at high risk for liver failure and HCC.[1–6] Thus, it is important to efficiently identify patients at risk for advanced fibrosis among a large number of NAFLD patients. In addition, differentiation of early-stage NASH allows for early intervention, which can improve patients' outcomes. Liver biopsy is the most reliable method for the diagnosis and determination of fibrosis stage in patients with NASH. However, it is

widely acknowledged that biopsy is costly and runs the risk of sampling error and procedure-related morbidity and mortality. Some guidelines recommend that liver biopsy should be considered in patients who are at risk for NASH with advanced fibrosis,[4–6] but this recommendation is not universally accepted. Therefore, various parameters have been proposed as tools to distinguish NASH from NAFLD, or to determine fibrosis stage. Various serum biochemical markers, including indicators of oxidative stress, insulin resistance, inflammation, and apoptosis, have been used for this purpose.[1–6]

With regard to glucose metabolism and insulin resistance, a 75-g OGTT may help clinicians to identify high-risk patients for more intensive monitoring and treatment because blood glucose and insulin levels in the OGTT are important factors for the diagnosis of NAFLD and prediction of fibrosis.[11,12,24–26] Studies in which a 75-g OGTT was performed have shown that impaired glucose tolerance is common even in NAFLD patients without overt DM,[11,12,24–26] and that postprandial hyperglycemia is associated with advanced fibrosis.[12,24,26] Postprandial hyperinsulinemia is also observed in nearly all NAFLD patients, even those with normal glucose tolerance.[11,12] Kimura *et al.*[11] reported that postprandial hyperinsulinemia, as indicated by an OGTT, became more marked as fibrosis stage advanced.

Indirect calorimetry provides important information about energy expenditure, npRQ, and the rate of oxidation of three major macronutrients (carbohydrates, fat and protein) based on respiratory gas exchange and urinary nitrogen excretion. Indirect calorimetry is considered the gold standard for assessing energy expenditure and aids in the delivery of the highest quality of nutritional care.[7] The advantages of this modality are that it is non-invasive, portable enough to be done at bedside, easy to operate and inexpensive.[7] Many studies have used this modality to estimate the nutritional state of cirrhotic patients with chronic liver disease. Tajika *et al.*[8] have reported that low npRQ derived from PEM is associated with survival in patients with viral liver cirrhosis. We have previously used indirect calorimetry in cirrhotic patients to evaluate the effects of nutritional treatment with branched-chain amino acids.[19,27–29] In diabetic patients, indirect calorimetry is often used to estimate glucose oxidation rate and it has been reported that both glucose oxidation and non-oxidative disposal are impaired during hyperinsulinemic clamping in type 2 DM patients.[30] Although indirect calorimetry is used for assessment in several metabolic diseases, this is the first report to examine indirect calorimetry data from patients with NAFLD. The objective of the present study was to determine how energy metabolism, as estimated by indirect calorimetry, is related to the clinicopathogenesis of NAFLD with glucose intolerance.

We found that npRQ decreased in severity with increased fibrosis stage in NAFLD patients. This observation raised the question of the mechanism underlying decreased npRQ in patients with advanced fibrosis. As fibrosis progressed, npRQ decreased significantly, glucose intolerance worsened and insulin resistance increased (Tables 2,3). In fact, negative correlations were seen between npRQ and several parameters of glucose intolerance: AUC glucose, HOMA-IR, and fasting glucose and insulin levels. Thus, we speculated that decreased npRQ in NAFLD results from glucose intolerance due to insulin resistance, which worsened with fibrosis stage. Decreased npRQ can reflect reduced glucose oxidation and enhanced lipid oxidation.[8,19,27–29] It was reported that peripheral insulin resistance reduces glucose oxidation and glucose uptake in peripheral skeletal muscle.[30] This reduction in glucose uptake may reflect hyperglycemia and decreased glucose oxidation, because the amount of free cellular glucose available for oxidation is reduced.[31] However, it was also speculated that the low glucose oxidation rate seen in viral cirrhosis is a result of reduced glucose production due to decreased hepatic glycogen.[32] In our study, glycogen levels in the liver were not measured directly and thus a definitive statement cannot be made. However, npRQ was low even in the one patient with mild (stage 1) fibrosis, who was found not to be in a state of malnutrition as determined by anthropometry and in whom glycogen storage was likely not decreased to a large extent. Therefore, it is unlikely that the low npRQ in these patients primarily reflects decreased glycogen stores. However, we do not suggest that low npRQ in NAFLD patients is solely due to glucose intolerance because whole-body energy metabolism is a complex process, and thus it is possible that other factors also contribute to low npRQ.[30] Yokoyama *et al.*[33] have reported that the glucose oxidation rate of subjects with type 2 diabetes is inversely correlated with BMI, body fat percentage and plasma fatty acid levels, suggesting that decreased glucose oxidation and increased fat oxidation may be potently affected by adiposity. In our study, npRQ showed no correlation with lipid parameters, including serum total cholesterol, triglyceride and NEFA, or anthropometric parameters such as body fat percentage and VFA. Thus, low npRQ was speculated to be associated with decreased glucose oxidation due to glucose intolerance, but not with increased fat oxidation, which occurs in the maintenance and development